STEPWISE STRATEGY TO CYCLOMETALLATED Pt(II) COMPLEXES WITH *N*-HETEROCYCLIC CARBENE LIGANDS. LUMINESCENCE STUDY ON NEW β–DIKETONATE COMPLEXES

Sara Fuertes,[†a] *Hector García,*[a] *Mariano Perálvarez,*[b] *Wim Hertog,*[b] *Josep Carreras,*[b] *Violeta Sicilia,**[c]

[a] Instituto de Síntesis Química y Catálisis Homogénea (ISQCH), CSIC - Universidad de Zaragoza, Departamento de Química Inorgánica, Facultad de Ciencias, Pedro Cerbuna 12, 50009, Zaragoza (Spain)

[b] IREC, Catalonia Institute for Energy Research. Jardins de les Dones de Negre 1. PL2, 08930 Sant Adrià de Besòs, Barcelona, Spain

[c] Instituto de Síntesis Química y Catálisis Homogénea (ISQCH), CSIC - Universidad de Zaragoza, Departamento de Química Inorgánica, Escuela de Ingeniería y Arquitectura de Zaragoza, Campus Río Ebro, Edificio Torres Quevedo, 50018, Zaragoza (Spain). E-mail: sicilia@unizar.es

[†] *ARAID Researcher*

ABSTRACT

The imidazolium salt 3-methyl-1-(naphthalen-2-yl)-1*H*-imidazolium iodide (**2**) has been treated with silver(I) oxide and [{Pt(μ-Cl)(η^3-2-Me-C_3H_4)}$_2$] (η^3-2-Me-C_3H_4 = η^3-2-methylallyl) to give the intermediate N-heterocyclic carbene complex [PtCl(η^3-2-Me-C_3H_4)(HC^C*-κC*)](**3**) (HC^C*-κC*= 3-methyl-1-(naphthalen-2-yl)-1*H*-imidazol-2-ylidene). Compound **3** undergoes a regio-specifically cyclometallation at the naphthyl ring of the NHC ligand to yield the five-membered platinacycle compound [{Pt(μ-Cl)(C^C*)}$_2$] (**4**). The chlorine abstraction of **4** with β-diketonate Tl derivatives rendered the corresponding neutral compounds [Pt(C^C*)(L-*O,O'*)] (L = acac (HL = acetylacetone) **5**, phacac (HL= 1,3-diphenyl-1,3-propanedione) **6**, hfacac (HL= hexafluoroacetylacetone) **7**). All of them (**3**-**7**) were fully characterized by the usual spectroscopic and analytical methods. X-ray diffraction studies were performed on **5**-**7**, revealing short Pt-Pt and π -π interactions in the solid state structure. The influence of

the R-substituents of the β-diketonate ligand on the photophysical properties has been studied and also the use of the most efficient emitter, **5** as phosphor converter.

INTRODUCTION

Solid-State Lighting (SSL) is now a mature technology that is rapidly climbing in share among the different commercial lighting technologies.[1] Nowadays, two main strategies are available within state-of-the-art SSL to generate white luminescence. On one hand, there are the so-called PC-LEDs (phosphor-converted LED) based on high efficiency blue LEDs combined with green, yellow and/red phosphors. In these devices, short-wavelength emission from the LED dye is partially downconverted by the phosphors. White light results then from the combination of the phosphors re-emission and LED non-absorbed light. The second approach, the RGB LED, consists of three emitters (primary at around 455nm, 530nm and 610nm) packaged closely together to form a compact semiconductor light source with a tunable chromaticity point. However, most of general lighting applications are dominated by PC-LEDs, because of its several advantages. First, the efficiency of direct electroluminescence exhibits important variations across the visible spectrum. Whereas current external quantum efficiency is around 75 % in the blue range and 64 % in the red, the efficiencies at the green and amber ranges are 32 % and 11 %, respectively .[2] Thus, at least for green and yellow light, it is more efficient to obtain these contributions under the PC strategy. Second, PC-LEDs are far less sensitive to temperature than LEDs, allowing simpler (and cheaper) control strategies in order to maintain device chromaticity.

Phosphors used in mainstream LED technology are typically inorganic, comprising a crystalline oxide, nitride, oxynitride or silicate host lattice, doped with a small dose of an activator ion, in most cases rare earths. Ce^{3+} and Eu^{2+} are the activator ions more broadly used in SSL and it is just here where it is foreseen that PC-LEDs can have a potential weakness in the next decade since the global shortage of these materials is currently having a direct impact on phosphor availability and pricing.[3] In the light of this, it is clear the necessity of new approaches and materials capable of replacing in the next future these rare-earth based phosphors.

At this point, platinum (II)-based phosphorescent complexes have been attracted much interest due to their potential use as dopants in LEDS,[4] chemical sensors[5] or bio-labeling agents,[5b, 6] with special attention being paid to C^N-cyclometallated

derivatives.[4b, 7] The strong ligand field induced by the C-σ bond (σ donor) and the aromatic fragment (π acceptor) characteristics of the C^N-ligands enhance the splitting of the d orbitals. Consequently, the energy of the non-radiative excited states (d-d) on the metal centered is raised, avoiding the thermal quenching. Hence, the incorporation of strong field ligands to the metal coordination sphere is one of the key requirements, among others, for the design of these phosphorescent systems. Bearing this in mind, the cyclometallated N-heterocyclic carbenes (NHC) may surpass the high ligand field splitting capacity of the C^N-ligands, since they present two C-σ bonds. This implies an even greater heightening of the d-d energy levels on the metal center, enlarging the energy gap with the emissive excited states and improving the quantum yields.[8] Another consequence of the presence of strong carbon-metal bonds is the robustness and/or stability of the carbene complexes which may provide long-term functional materials.

NHC carbenes have been widely used in organometallic chemistry and particularly in the targeted fields of transition-metal catalysis,[9] liquid crystals,[10] bio-medicine,[11] and luminescence materials.[8, 11d, 12] However, phosphorescent compounds of platinum(II) containing cyclometallated NHC ligands have been barely explored with only a handful of reports published very recently.[13] Moreover, most of them contain the chelate *β*-diketonates or *β*-ketoiminates as ancillary ligands, and have been prepared following a restricted one-pot synthetic route which renders exclusively and straightforward these derivatives.[13b, 13c, 13e-i, 14] As stated by the authors,[13i] the synthesis has its difficulties and renders rather low yields (~30%[13c, 13e, 13f, 13i] or < 50%[13g, 13h]). The introduction of different kinds of ancillary ligands in the coordination environment of the metal centre plays a major role in the design of phosphorescent complexes, because, tuning of emission colors over the entire visible spectra is achieved by modification of the cyclometallated and/or the ancillary ligands.[4b, 7a, 15] The electronic nature of the ligands affects the electron density at the metal center and their steric requirement can preclude the existence of metal-metal or π-π interactions which consequently alter the relative energy, radiative color, and lifetime of the excited state.[15e, 16] As part of our preceding research, we have studied this influence spectroscopically and structurally in heteroleptic complexes of Pt(II) with the 7,8-benzoquinolinato and different monodentated auxiliary ligands such as alkynyls, nitriles, chlorides, cyanides and isocyanides.[16a, 17]Keeping on with our previously described stepwise protocol to

prepare C^N-cyclometallated of platinum (II) complexes,[18] we tried this same synthetic approach using the N-heterocyclic carbene as a cyclometallated ligand. The anchoring of the NHC ligand through the carbene carbon atom to the platinum center will allow the following C-H activation at the aromatic substituent to afford a NHC cycloplatinated species.Thus, in this manuscript, we describe for the first time the use of [{Pt(μ-Cl)(η^3-2-Me-C_3H_4)}$_2$] to achieve a stepwise cyclometallation by isolating the intermediate carbene complex [PtCl(η^3-2-Me-C_3H_4)(HC^C*-κC*)]. This will subsequently undergo a second C-H activation to lead the cycloplatinated complex [{Pt(μ-Cl)(C^C*)}$_2$]. Therefore, having access to a generic precursor such as [{Pt(μ-Cl)(C^C*)}$_2$], where the chlorine atom can be easily removed, enables a facile and resourceful strategy to prepare heteroleptic complexes [Pt(C^C*)LL'] containing the cycloplatinated NHC moiety. Only for comparative purposes with previously reported results,[13b, 13c, 13e-g, 13i] we have prepared a series of β-diketonates derivatives [Pt(C^C*)(L-*O,O'*)] (L = acac (HL = acetylacetone) , phacac (HL= 1,3-diphenyl-1,3-propanedione), hfacac (HL= hexafluoroacetylacetone)) and the use of the most efficient emitter among them (L = acac, phi = 53%) as phosphor converter has been also studied.

RESULTS AND DISCUSSION

Preparation of NHC Ligand. Synthesis and Characterization of [PtCl(η^3-2-Me-C_3H_4)(HC^C*-κC*)](3) (HC^C*-κC*= 3-methyl-1-(naphthalen-2-yl)-1*H*-imidazol-2-ylidene)

The synthesis of the N-heterocyclic carbene precursor is prepared by a modified Ullmann- type condensation (Scheme 1a). Following a slightly different method to that of Xu and coworkers,[19] 2-bromonaphthalene was coupled with imidazole in DMSO at 110ºC using copper(I) oxide and potassium hydroxide. After work-up, the mixture was purified by column chromatography on silica gel using ethyl acetate / methanol (9:1) as eluent to give 1-(naphthalen-2-yl)-1*H*-imidazole (**1**) in good yield (67%). This imidazole derivative was previously prepared in relatively good yields (54%[20] and 80%[21]) but it required harsh reaction conditions (170ºC) and the use of high (non-catalytic*)* amounts of diamine ligands (N,N'-dimethylethylenediamine and 1,10-phen). Then, methyl iodide was added to a refluxing THF solution of **1** to give the corresponding imidazolium salt: 3-methyl-1-(naphthalen-2-yl)-1*H*-imidazolium iodide (**2**) (see Scheme 1b and Experimental Section).

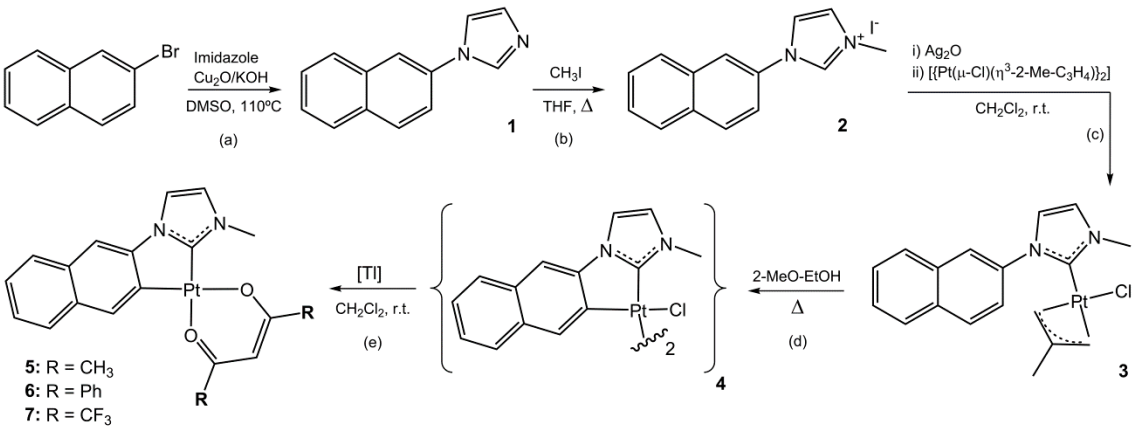

Scheme 1. Synthesis of compounds **1**-**7**

Keeping on with our previously described stepwise protocol to prepare C^N-cyclometallated complexes of platinum (II),[18] we tried this same procedure using the N-heterocyclic carbene. The imidazolium salt was reacted with silver(I) oxide to give the corresponding NHC carbene complex of silver which was not isolated. Upon addition of the dichloro-bridged complex [{Pt(μ-Cl)(η^3-2-Me-C_3H_4)}$_2$] (η^3-2-Me-C_3H_4 = η^3-2-methylallyl) to the mixture, a yellow precipitated (AgI) was immediately observed, as a result of the transmetalation from Ag(I) to the Pt(II) center. After work-up the mixture, the neutral complex [PtCl(η^3-2-Me-C_3H_4)(HC^C*-κC*)](**3**) was isolated as a pale yellow and air stable solid in very good yield (75%). In the IR spectrum, an absorption band at 280 cm^{-1} was attributed to υ_{Pt-Cl} which is consistent with a terminal Pt-Cl bond in *trans* disposition to a ligand with a large *trans* influence as η^3-2-Me-C_3H_4.[18a]

Unfortunately, all attempts to obtain single crystals of **3** failed; however, the new compound was fully and unequivocally characterized by multinuclear NMR spectroscopy. ^{1}H and ^{13}C NMR signals were clearly identified by ^{1}H-^{1}H and ^{1}H-^{13}C correlations; The number of signals and their relative integrals are in agreement with the formulation proposed and the lack of symmetry in complex **3** (see Figure 1 and S1 in S.I.). It can be noticed that the singlet at 9.88 ppm, which was attributed to H1 in the free ligand, has completely disappeared. The H2 and H3 protons of the imidazolyl moiety appear upfield shifted and show Pt satellites with Pt-H coupling constants of *ca.* 10 Hz. The resonances corresponding to the naphthalene moiety are displayed in two sets of multiplets and do not show any coupling to the platinum center.

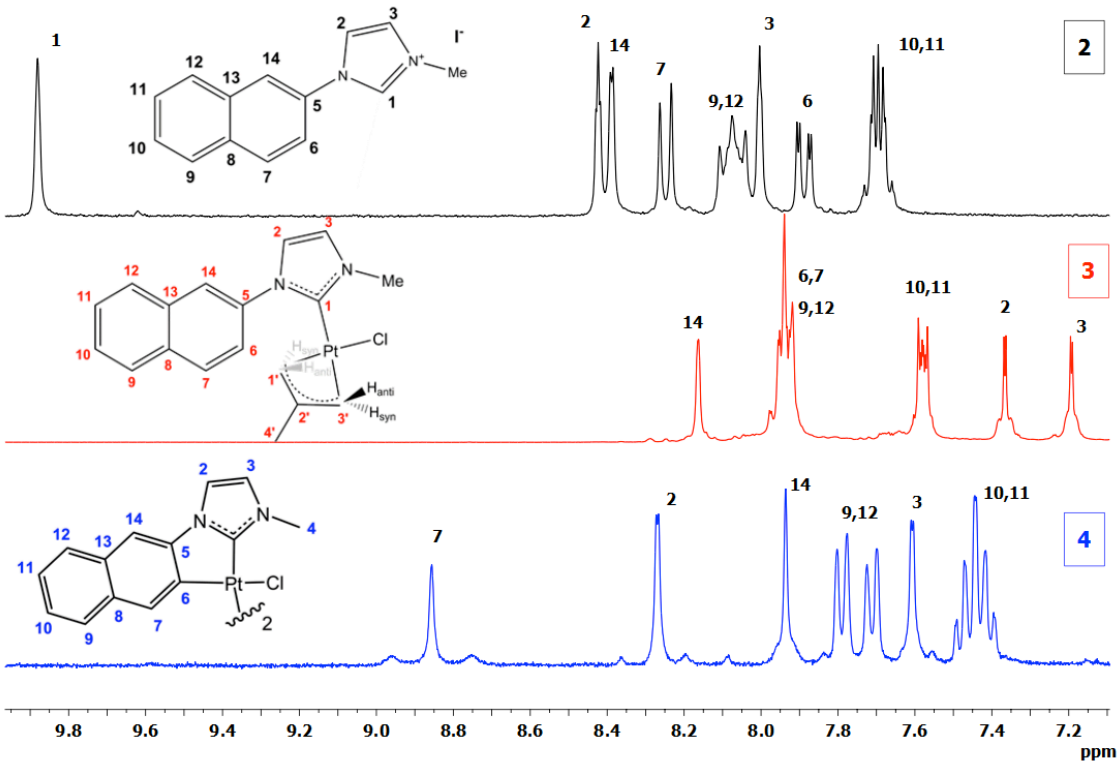

Figure 1. ^{1}H NMR spectra of **2** (DMSO-d^6), **3** (CD_2Cl_2) and **4** (DMSO-d^6) at r. t.

The methyl allyl group (η^3-2-Me-C_3H_4) gives the expected ^{1}H and ^{13}C NMR signals with values of $J_{Pt\text{-}H}$ and $J_{Pt\text{-}C}$ slightly smaller to those found in the η^3-allyl derivatives [{Pt(μ-Cl)(η^3-2-Me-C_3H_4)}$_2$][22] and [Pt(η^3-C_4H_7)Cl(HC^N-κN)] (HC^N = 2-(4-bromophenyl)imidazol[1,2-a]pyridine),[18a] as expected for the stronger *trans* influence of a C (NHC) with respect to a Cl or N, respectively. The ^{13}C1 resonance appears at 176.4 ppm and the ^{195}Pt{^{1}H} resonance at -4457 ppm, in the same spectral region to the analogous complex [Pt(η^3-C_4H_7)Cl(HC^N-κN)].[18a] All these spectroscopic features indicate the success of the trans-metalation to the Pt center.

Cyclometallation of 3. Synthesis and Characterization of [{Pt(μ-Cl)(C^C*)}$_2$] (4).

When a suspension of **3** in 2-methoxyethanol was refluxed for 4h, it turned into a dark-greyish mixture. Recrystallization of the filtrated solid in hot acetonitrile solution (see Scheme 1d and Experimental Section) rendered **4** as a pure white solid in reasonably good yield (60%), considering the cyloplatination process. The cyclometallation could be carried out at two non-equivalent positions of the *beta*-substituted naphthalene: *alfa* and *beta*, C14 and C6, respectively; (see Figure 1 for numeration) to form two different five-membered rings. Although the *beta*-position is the thermodynamically favored site

for electrophilic attack,[23] the *alfa*-position is kinetically favored.[24] A naphthalene system *beta*-substituted with an electron-donating group usually directs the reaction kinetically to the *alfa*-position of the same ring, due to the more effective delocalization of the positive charge in the carbocation intermediate formed on the attack.[25] However, the C-H activation took place regio-specifically at the *β*-position (C6), since this metallation site is less hindered, as reported before.[26] No other by-products were detected from the reaction mixture.

The new dichloro-bridged cycloplatinated compound [{Pt(μ-Cl)(C^C*)}$_2$] (**4**) was fully and unambiguously characterized by NMR spectroscopy. All NMR experiments of **4** were recorded in DMSO-d_6, because of its low solubility in other common solvents and the signals were assigned on the basis of a ^{1}H-^{1}H and ^{1}H-^{13}C experiments (see Experimental Section and Figures 1 and S2). The ^{1}H spectrum confirmed the absence of the allyl group and the metalation of the 3-methyl-1-(naphthalene-2-yl)-1*H*-imidazol-2-ylidene) (HC^C*-κC*) through the *β*-C of the naphthyl ring (C6), since two isolated singlets, assigned to H7 and H14, were observed at 8.85 and 7.93 ppm, correspondingly. Besides, the H7 proton displays Pt satellites with a Pt-H coupling constant of *ca* 63 Hz. The H2 and H3 protons of the imidazolyl are slightly downfield shifted with respect to those of **3** and barely any Pt-H couplings were observed. The ^{13}C1 resonance appears at 156.1 ppm which is in good agreement with the literature values.[13b, 13e-h, 27]

Up to date, the two-step process, coordination and subsequent cycloplatination of N-heterocyclic carbene ligands has been only reported with the compound [PtMe$_2$(DMSO)$_2$].[28] In this paper, we describe for the first time the use of the chloro-bridge complex [{Pt(μ-Cl)(η^3-2-Me-C$_3$H$_4$)}$_2$] to achieve this stepwise cyclometallation by isolating the intermediates. Unlike what has been recently stated,[13i] we have been able to prepare and characterize the intermediate complex (compound **3**), that subsequently undergoes a regio-specifically cyclometallation of the coordinated NHC carbene. As part of our ongoing research on this stepwise procedure, very promising results using different N-heterocyclic carbene ligands endorse the generality of this step by step protocol using the [{Pt(μ-Cl)(η^3-2-Me-C$_3$H$_4$)}$_2$] complex to prepare new NHC precursors, [{Pt(μ-Cl)(C^C*)}$_2$] (unpublished results). If we compare the final products of the carbene cyclometallation, using the DMSO-derivative, [Pt(C^C*)(DMSO)Me],[28] with ours, [{Pt(μ-Cl)(C^C*)}$_2$] (**4**), it seems clear that our system presents a significant advantage over the other. Whilst the DMSO-derivative has a methyl group and a

molecule of DMSO in the coordination sphere of the platinum, which none of them are labile ligands to be replaced, in [{Pt(μ-Cl)(C^C*)}$_2$], the chlorine atom can be easily removed obtaining the "Pt(C^C*)" fragment with two vacant coordination sites available to be occupied by different kinds of ancillary ligands. Therefore, these systems, [{Pt(μ-Cl)(C^C*)}$_2$], offer a more versatile and accessible pathway to prepare heteroleptic complexes [Pt(C^C*)LL'] which enhance the possibilities of modulating the electronic properties of the metal center and consequently its emissive behaviour. As far as we know, most of the photoluminescence studies and synthetic methods of NHC cycloplatinated chelate compounds were restricted to the diketonate derivatives.[13b, 13c, 13e-i, 14] Only for comparative purposes with former reported results,[13b, 13c, 13e-g, 13i] we have prepared a series of new β-diketonates derivatives.

Synthesis and Characterization of [Pt(C^C*)(L-*O,O'*)] (L = acac 5, phacac 6, hfacac 7)

The reaction of the chlorine bridged compound **4** with the corresponding thallium (I) salts in 1:2 molar ratio (see Scheme 1 and Experimental Section) led to the precipitation of TlCl and formation of the neutral complexes [Pt(C^C*)(L-*O,O'*)] (L = acac **5,** phacac **6,** hfacac **7)** which are obtained from the solution as white (**5**), yellow (**6**) and orange (**7**) air-stable solids in good yields. The υ(C=O) stretching vibrations appear at significantly lower energies than those found for the free ligands (*ca*.1720 cm^{-1}) and are indicative of the diketonate chelation to the metal center.[29] The non-equivalence of the two halves of the β-diketonate ligands, expected for chelate coordination, is evident from the ^{1}H, ^{19}F and ^{13}C NMR spectra (see Experimental Section and Figures S3a, S3b, and S3c). The ^{1}H resonances corresponding to the NHC carbene are very similar in all three complexes (see Figure S3a), except for H7, which seems to be rather sensitive to the nature of the ancillary ligand (L-*O,O'*). It appears as a singlet at 8.06 ppm with a Pt-H coupling constant of 57 Hz for compound **5**, whilst for **6** and **7** it is shifted to downfield (8.25 ppm) and upfield (7.79 ppm), respectively. The ^{195}Pt{^{1}H} spectra registered in CD_2Cl_2-d^2 for **5**-**7** exhibit the corresponding singlets at -3360, -3296 and -3232 ppm, which are characteristic for this type of complexes.[13e-g, 30] As shown in Figure S4, the platinum signal is less shielded in **6** and **7** when compared to that of **5**, probable due to the more electron withdrawing character of the β-diketonate ligands.

The crystal structures of **5-7** have been determined by X-ray diffraction studies (Figures 2-4, Table S1). Compound **6** crystallizes in the noncentrosymmetric orthorhombic $P2_12_12_1$ space group. The asymmetric unit contains two molecules (Pt01 and Pt02) with similar structural details (see Figure 3). In all three complexes, the platinum(II) center exhibits a distorted square-planar environment due to the small bite angle of the NHC cyclometallated ligand (C^C*) [80.26(11) - 80.90(2)°]. A chelate diketonate ligand, with O-Pt-O angles close to 90 degrees, completes the coordination sphere of Pt(II). The Pt-C_{NHC} bond lengths [1.928(5) – 1.946(3) Å] are shorter than those observed for the Pt-C_{Naph} [1.974(3) – 1.986(5) Å]. These structural data together with the Pt-O distances [2.040 - 2.116 Å] are similar to those found in related complexes.[13b, 13c, 13e-g, 13i]

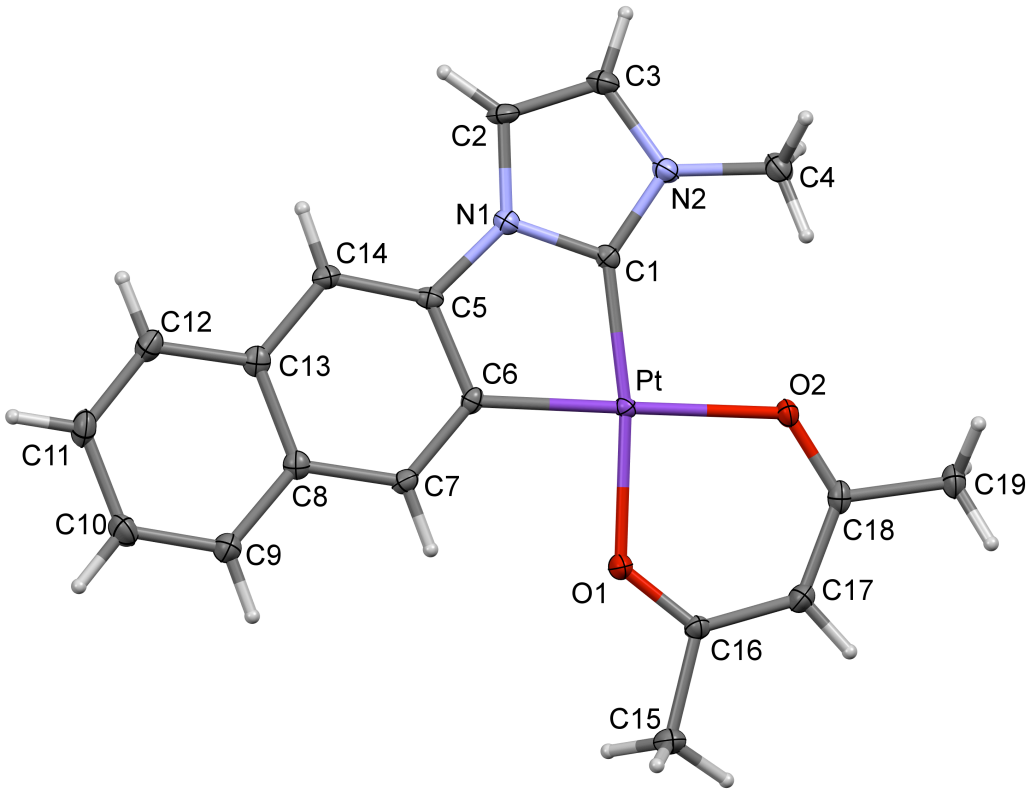

(a)

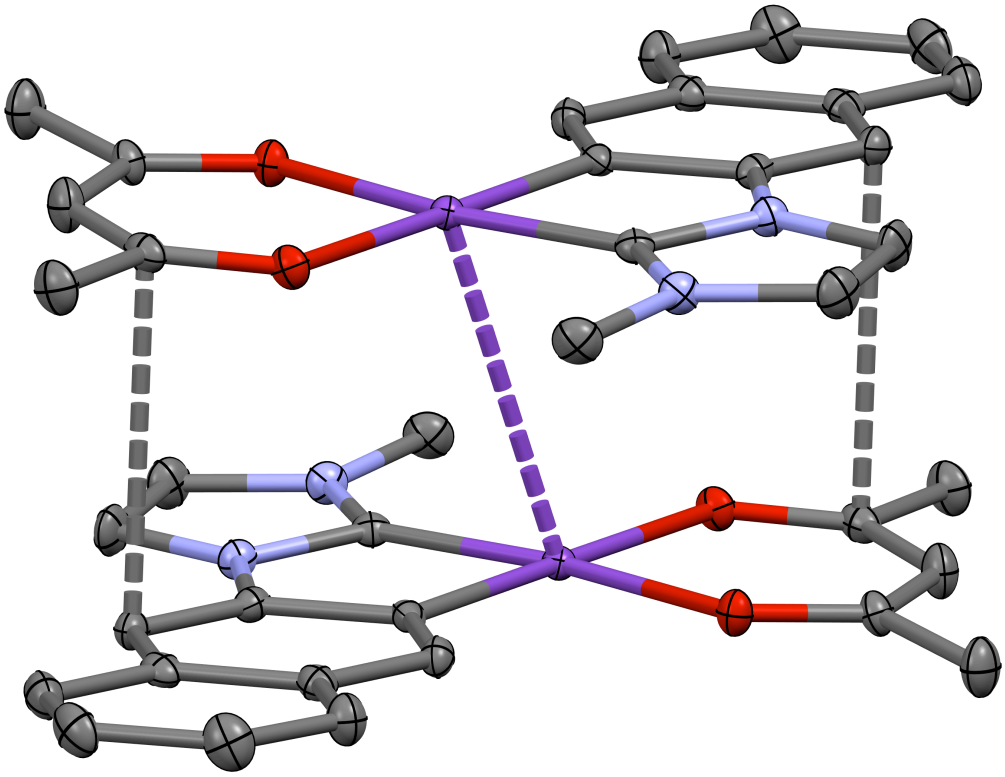

(b)

Figure 2. a) ORTEP view of **5·0.5CH_2Cl_2**. Thermal ellipsoids are drawn at the 50% probability level. Selected bond lengths (Å) and angles (deg): Pt-C(1) 1.946(3); Pt-C(6) 1.980(2); Pt-O(1) 2.0440(19); Pt-O(2) 2.0918(18); C(1)-Pt-C(6) 80.85(11); O(1)-Pt-O(2) 90.00(7). b) Stacking arrangement in a dimer-like fashion. Solvent molecules and hydrogen atoms have been omitted for clarity. Distance of Pt-Pt = 3.392 Å.

Complexes **5** - **7** are practically planar, the dihedral angles between the platinum coordination planes [Pt, C1, C6, O1, O2; Pt02, C30, C35, O3, O4 (Figure 3)] and the naphthyl moieties [C5-C14; C34-C43] are 3.99º (**5**), 3.45º, 5.05º (**6**) and 1.48 º (**7**).[31] Also, the angles between the Pt coordination plane and the imidazol moieties [C1, N1, C2, C3, N2; C30, N3, C31, C32, N4] are 1.61º (**5**), 3.45º, 2.56º (**6**) and 4.57 º (**7**).[31] The ligand NHC carbene cyclometallated itself is not completely planar; it exhibits small interplanar angles between the naphthyl and the imidazol fragments are 5.14º (**5**), 4.24º, 5.67º (**6**) and 3.67 º (**7**).[31] Likewise, the dihedral angles between the diketonate ligands and the Pt coordination planes are 3.93º(**5**), 11.19º and 1.29º (**6**) and 1.41º (**7**). As inferred from these data, the diketonate ligand of the Pt01 molecule in **6** is evidently

bent out of the Pt01 coordination plane with the C50, C57 and C58 atoms at a distance of 0.291(5), 0.413(5) and 0.218 (4) Å.

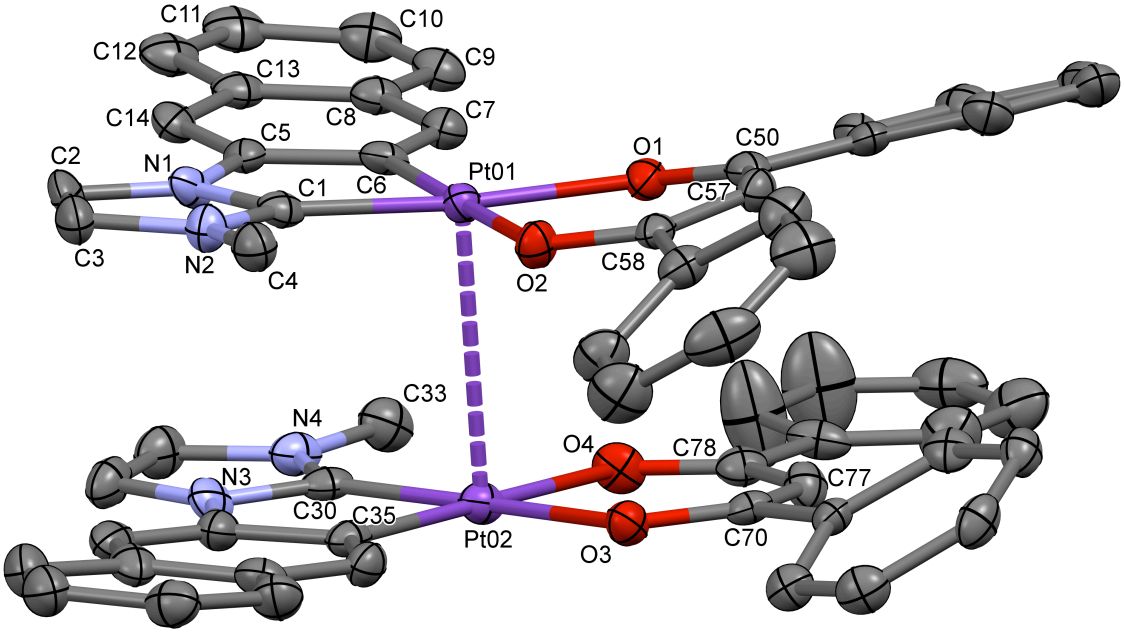

Figure 3. ORTEP view of **6**. Thermal ellipsoids are drawn at the 30% probability level. Hydrogen atoms have been omitted for clarity. Selected bond lengths (Å) and angles (deg): Pt(01)-C(1) 1.928(5); Pt(01)-C(6) 1.986(5); Pt(01)-O(1) 2.047(4); Pt(01)-O(2) 2.065(3); Pt(02)-C(30) 1.944(5); Pt(02)-C(35) 1.980(5); Pt(02)-O(3) 2.040(3); Pt(02)-O(4) 2.090(4); C(1)-Pt(01)-C(6) 80.90(2); O(1)-Pt(01)-O(2) 89.45(13). C(30)-Pt(02)-C(35) 80.90(2); O(3)-Pt(02)-O(4) 89.73(14). Distance of Pt(01)-Pt(02) = 3.254 Å.

In the solid state crystal structure packaging, complex **5** arranges together in pairs, in a head to tail fashion through intermolecular Pt-Pt (3.392 Å) and π - π (~ 3.35 Å) interactions between the NHC ligand and the acac (See Figure 2b).[13c, 13e, 32] Compound **6** crystallizes as a dimer; both halves consist of a square–planar "Pt(C^C*)(L-*O,O'*)" moiety held together by a rather short Pt-Pt interaction (3.254 Å), which is below than the sum of the van der Waals radii.[33] In this case, the molecules arrange themselves in a head-to-head fashion, showing a clear offset stacking (torsion angle C(1)−Pt(01)−Pt(02)−C(35): 31.5(2)°; see Figure S5), that minimizes the steric repulsion of the ligands and enhances the Pt···Pt and π···π interactions.[34] The phacac ligands are lying on top of each other whereas the NHC ligands are flipped over, leading to π -π (~ 3.37 Å) interactions between the imidazole and the naphthyl systems. The platinum

coordination planes are basically parallel to each other (interplanar angle 2.62(1)°) and the Pt(01)−Pt(02) vector is almost perpendicular to both platinum coordination planes (4.6(6)° Pt(01) and 5.9(7)° Pt(02)).

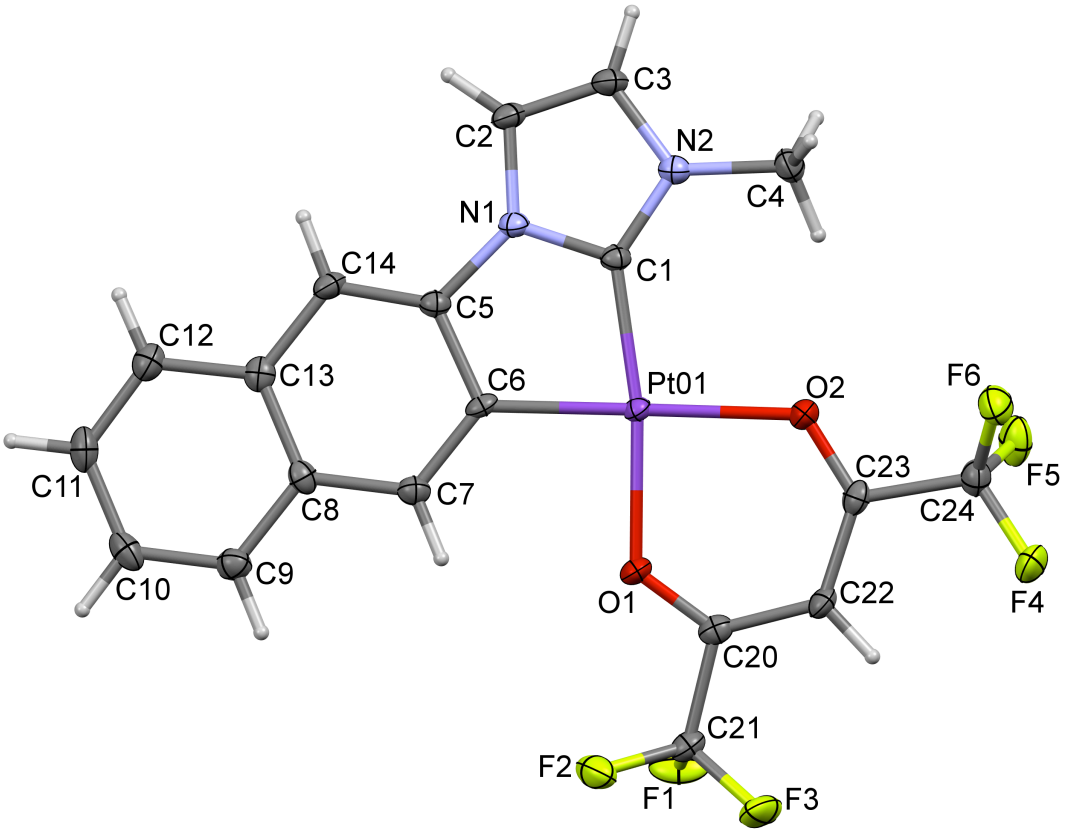

Figure 4. ORTEP view of **7**. Thermal ellipsoids are drawn at the 50% probability level. Selected bond lengths (Å) and angles (deg): Pt(01)-C(1) 1.943(3); Pt(01)-C(6) 1.974(3); Pt(01)-O(1) 2.050(2); Pt(01)-O(2) 2.116(2); C(1)-Pt(01)-C(6) 80.26(11); O(1)-Pt(01)-O(2) 88.79(8).

On the contrary to **5** and **6**, complex **7** does not exhibit short Pt-Pt interactions (~ 4.463 Å), however, the molecules stack into pairs in an offset head-to-tail fashion showing weak π -π (~ 3.7 Å) interactions between the imidazole and the naphthyl and acac systems (see Figure S6a). Also, the molecule exhibits some close C-H···F interactions with the neighbouring molecules (see Figure S6b. C(12)-H(12)···F(3); C(12)···F(3) = 3.18(3) Å; H(12)···F(3) = 2.46(2) Å; C-H···F = 143.97(2)°).

Photophysical properties of compounds 5-7

Absorption spectra and DFT calculations

UV-Vis spectra data of compounds **5-7** are listed in Table S2. As shown in Figure 5, they all display strong absorption bands at *ca*. 270 nm ($\varepsilon > 10^4$ $M^{-1}cm^{-1}$) which are normally attributed to the ^{1}IL transitions of the NHC ligand. Also, they show absorptions at around 300 nm together with weaker shoulders at 330-350 nm that, in the case of **7**, are evidently shifted to higher energies. According to the literature reports, these bands arise from a metal-to-ligand charge transfer (^{1}MLCT) transition.[13e-h] Additionally, compounds **6** and **7** show a broad absorption at around 380 nm ($\varepsilon \sim 10^3$ $M^{-1}cm^{-1}$). The absorption spectra of both complexes, **6** and **7**, at concentrations ranging from 10^{-3} to $5 \cdot 10^{-6}$ M (See Figure S7) showed that the absorptions at 372 (**6**) and 376 nm (**7**) obey Beer's Law, suggesting that they are due to transitions in the molecular species and no significant aggregation occurs within this concentration range.

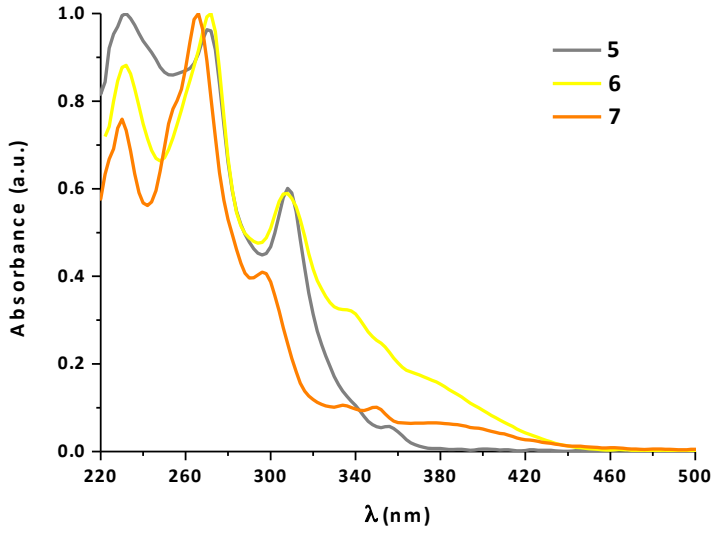

Figure 5. Normalized absorption spectra of **5-7** in CH_2Cl_2 ($5 \cdot 10^{-5}$ M).

UV-Vis spectra of **5-7** were recorded in different solvents showing a moderate negative solvatochromism, particularly more intense in the lower energy spectral region ($\lambda > 300$ nm). The absorption maxima suffer a blue shift of *ca* 6 nm when increasing the polarity of solvents (see Figure S8 for complex **6**), which is characteristic of charge transfer (CT) transitions.[35]

Solid state diffuse reflectance spectra of **5-7** are depicted in Figure 6. They show no significant differences when compared to those observed in solution of CH_2Cl_2.

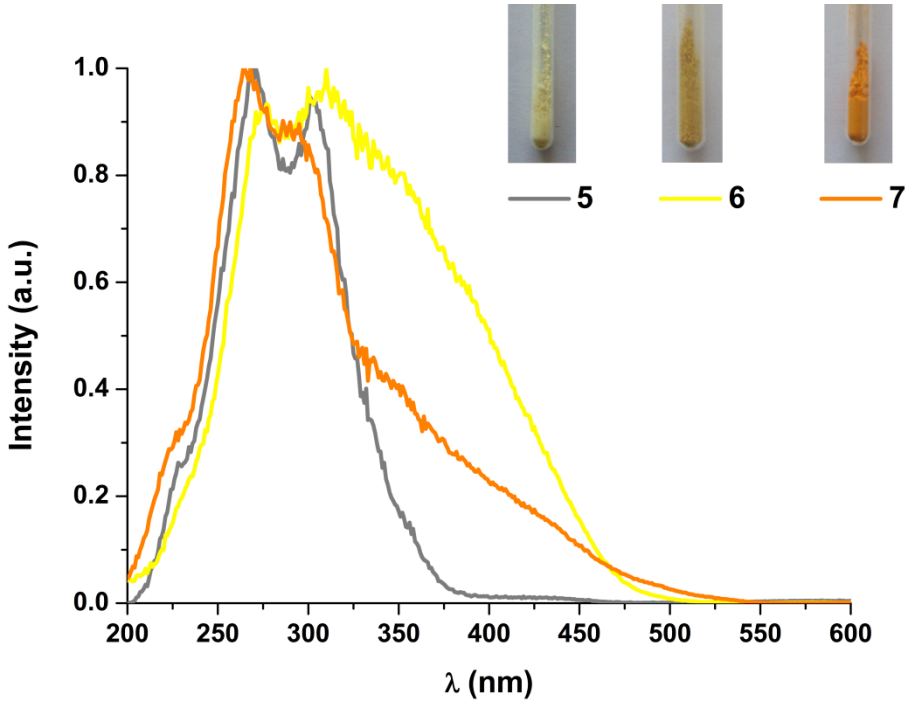

Figure 6. Normalized Diffuse Reflectance spectra of solid samples of **5-7** at r.t.

To better explain the UV-Vis assignments, time-dependent density functional theory (TD-DFT) calculations were carried out for **5-7** using the B3LYP hybrid density functional. The geometric parameters of the optimized structures (Tables S3 – S5) agree well with the experimental values. The molecular orbitals involved in the main excited states are depicted in Figures S9-S11 and the relative compositions of the different energy levels are reported in Table 1. Calculated excited states in solution of CH_2Cl_2 for complexes **5** - **7** are listed in Table 2. As can be seen, the highest occupied molecular orbital (HOMO) is mainly constructed from orbitals located on the Pt (21% **5**, 21% **6**, 16% **7**), the naphthyl group of the NHC ligand (69% **5**, 69% **6**, 81% **7**) and to a minor extent on the *β*-diketonate ancillary ligand (10% **5**, 10% **6**, 3% **7**). By contrast, the lowest unoccupied molecular orbital (LUMO) is well located on the *β*-diketonate moiety (74% **5**, 96% **6**, 95% **7**) and also on the NHC ligand (24%) for complex **5**.

The selected allowed transitions are in good agreement with the experimentally observed absorption maxima (Figures S12, S13 and S14). TD-DFT calculations on **5-7** indicate that there is a considerable orbital mixing for the transitions, particularly for compound **5**. The lowest energy calculated absorptions (S_1) for **5-7** are 338, 402 and 450 nm, respectively and they are involving the H → L transition. Therefore, they are attributed to mixed LL'CT [π(NHC) → π*(R-acac)]/ ML'CT [5d(Pt) → π*(R-acac)]

transitions and in the case of **5,** also, to ILCT [(NHC)]. These assignments are in concordance with other previously reported results.[13e, 13g, 13i] As stated by other authors,[13g] the additional rings at the R-acac ligand forms a π-extended system, which allows to a greater stabilization and a rearrangement of the LUMO composition in **6** (2% NHC / 96% phacac) compared to the one in **5** (24% NHC / 74% acac). This LUMO stabilization cannot be exclusively attributable to the formation of π-extended systems because it also happens with the electron withdrawing CF_3 groups in **7**. These stabilizations provoke a red shift in the lowest energy absorption of **6** and **7** with respect to that of **5**, as observed in the UV-Vis spectra; and it is also expected to give red-shifted emission bands.

Emission spectra

Complexes **5-7** are emissive in the solid state (298 and 77 K) and in glassy solutions (77 K) of 2-Methyltetrahydrofuran (2-MeTHF) but none of them are emissive in fluid solutions at room temperature (Table 3).

In diluted glassy solutions (10^{-5} M), compounds **5** and **6** show well-resolved vibronic emissions at high energy, see Figure 7, that do not change at higher concentration (10^{-3} M, Figure S15 and Table 3). These vibrational spacings [1174 - 1464 cm^{-1}] correspond to the C=C / C=N stretches of the cyclometallated NHC ligand (C^C*), suggesting the involvement of this in the excited states. Like the low energy absorption bands, the emission of **6** (λ_{max} 493 nm) is red shifted with respect to that of **5** (λ_{max} 474 nm), due to the greater stabilization of the LUMO, as revealed by the DFT studies. All excitation spectra are closely related to their corresponding UV-Vis spectra (Figure 5). Emission lifetimes measurements fit to one rather long component (408 μs (**5**) and 15 μs (**6**)). Therefore, from all these data, and considering the TD-DFT calculations, these high energy emissions are assigned to ^{3}LL'CT [π(NHC) → π*(R-acac)]/ ML'CT [5d(Pt) → π*(R-acac)] transitions, characteristics of monomeric species. The longer lifetimes measured for **5** could be explained by the additional contribution of the ^{3}ILCT (NHC) transition. The emissive behaviour of complex **7** is wavelength dependent. Upon excitation with λ_{ex} < 340 nm, it appears an emission band with maximum at 474 nm that is identical to that observed in **5**. However, when exciting with λ_{ex} > 360 nm this emission is almost disappeared, whereas a very weak and unstructured band appears at λ_{max} = 580 nm, to become the only one observed when the concentration is increased to 10^{-3} M (Figure S15 and Table 3). This concentration-dependent and weak low-energy

band (λ_{max} = 580 nm) displays a short lifetime measurement (~ 1.8 μs); also the excitation spectrum obtained monitoring this band, closely resembles the UV absorption spectrum. Because of that this emission has been attributed to excimers likely formed by interaction of an excited molecule with an adjacent ground-state one through π-π interactions,[17d, 17e, 35-36] in view of the molecular stacking observed in its X-ray structure (Figure S6).

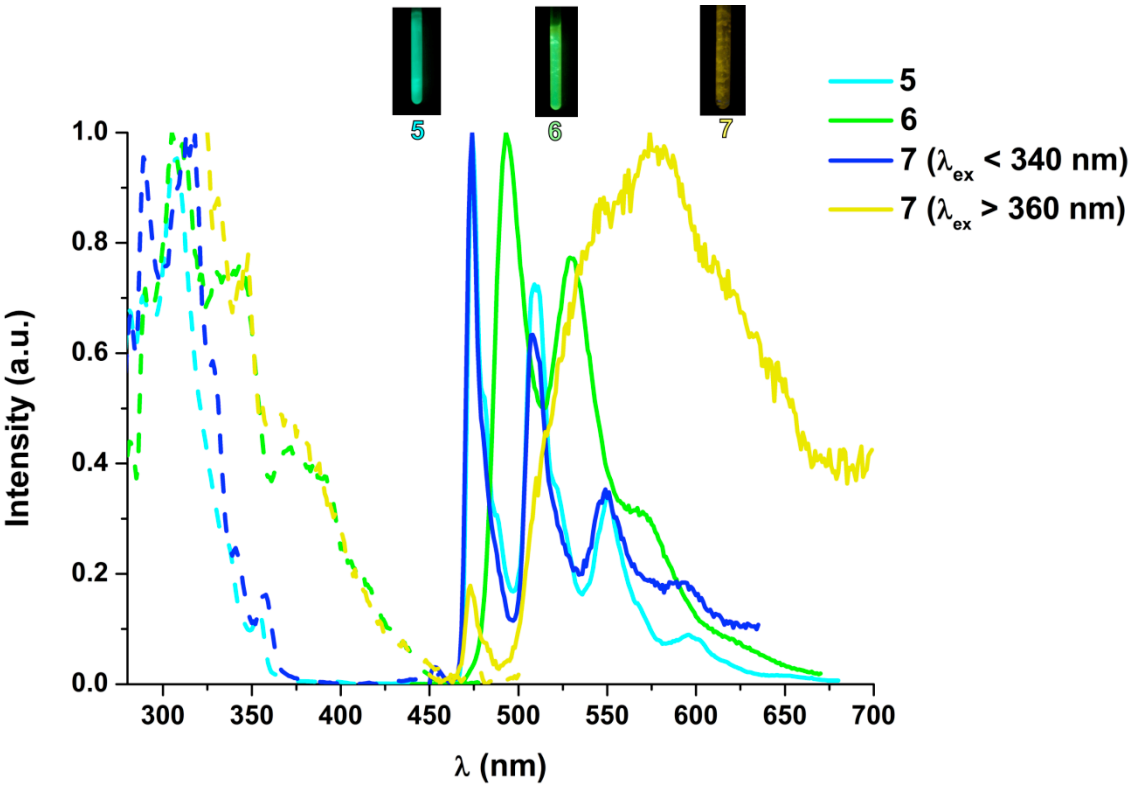

Figure 7. Normalized excitation (---) and emission (—) spectra of solutions of **5** - **7** in 2-MeTHF (10^{-5} M) at 77 K. Pictures of **5**-**7** taken with UV light (λ_{ex} = 365 nm).

In the solid state, complex **5** shows a green-yellowish band with maximum at 534 nm, see Figure 8. It presents a well-resolved vibronic pattern [1395 - 1458 cm^{-1}] that matches the skeletal vibrational frequency of the NHC ligand. This emission resembles to that obtained in solution, but rather shifted to lower energies. Therefore it is assigned to the same excited state. However, compounds **6** and **7** display rather different emission profiles, they appear as weak broad band at 680 nm and 608 nm, respectively (see Inset, Fig. 8) and whose excitation spectra (Figure 8) exhibit bands at lower energy than those observed in the diffuse reflectance spectra (Figure 6). Both emissions fit to short monoexponential decays (τ = 0.1 μs (**6**) and 0.3 μs (**7**)) and barely change upon

cooling to 77 K (Figure S16, table 3). Unlike related hfacac derivatives,[13g, 13i] complex **7** is slightly emissive in solid state at room temperature.

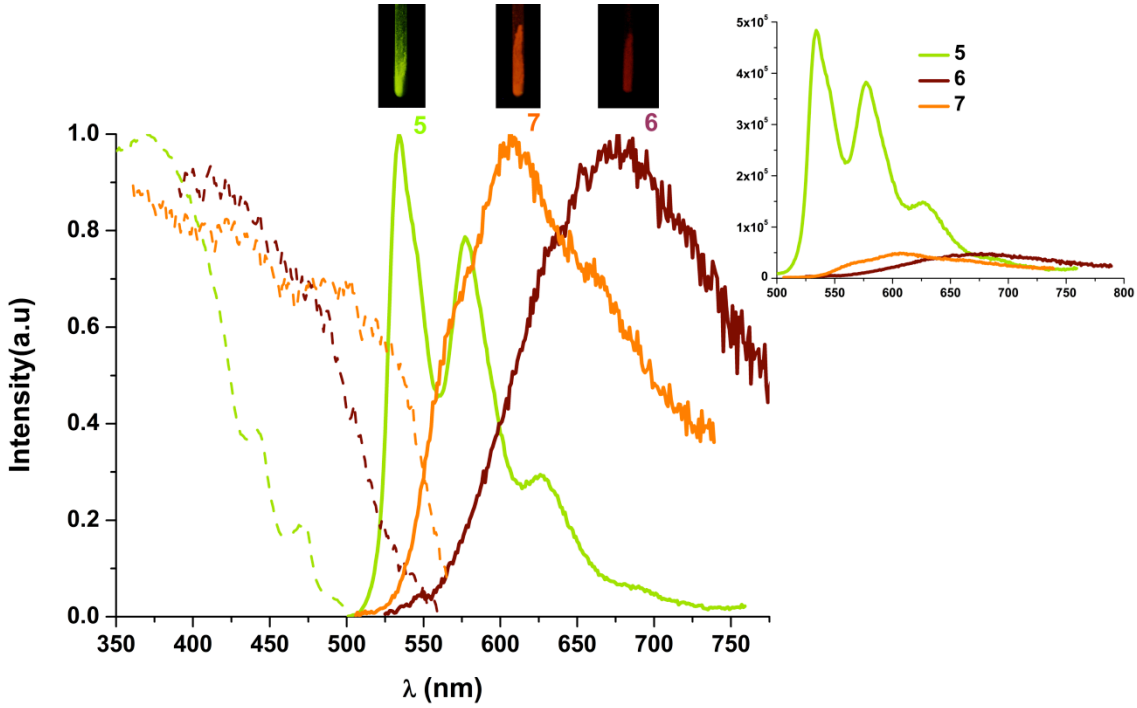

Figure 8. Normalized excitation (---) and emission (—) spectra of **5**-**7** in solid state at 298K. Inset: not normalized spectra. Pictures of **5**-**7** with UV light (λ_{ex} = 365 nm).

On the basis of band shape and energy, lifetime measurements and excitation spectra, the weak emission of **6** and **7** can be attributed to ^{3}MMLCT [dσ*(Pt) → π*] and/or $^3\pi\pi$* excited states in aggregates, in view of the Pt···Pt and /or π···π contacts observed in their X-ray structures (Figure 3, **6**; Figure S6, **7**).[16a, 17b, 17e, 37]

In light of the results shown in Figure 8, it becomes clear that such compounds could be suitable as down-converters for white LEDs implementation. On one hand, light absorption in the UV-blue spectral range makes them compatible with standard blue-LED pumping (the most efficient devices in the market). On the other, the broad emission in the green-yellow range turns these compounds into attracting alternatives for providing white luminescence, when properly combined with unabsorbed blue light.

However, to determine if these compounds are, indeed, suitable for implemented white LEDs further analyses are needed. First of all, it is mandatory to characterize how efficient are the phosphor in converting absorbed blue photons into lower energy photons. To do so, quantum yield (QY) measurements were carried-out on samples **5**, **6** and **7**. The study reveals that sample **5** exhibit the highest efficiency with values around 50 % in a broad range of excitation wavelengths (from 325 to 425 nm) and a maximum value of 53 % at 365 nm (see Table 3), comparable to those previously reported.[38] In samples **6** and **7**, in contrast, the exhibited re-emission is remarkably inefficient with values of ~1 (excitation range from 450 to 500 nm) and ~2 % (excitation range from 400 to 500 nm), respectively. It is worth noting how only by altering the electronic properties of the R-substituents in the ancillary ligand β-diketonate, the efficiency can experience this enormous quench. The thermo-gravimetric analysis (TGA) of **5** indicates that it is stable under argon at 1 atm to *ca* 300°C (Figure S17).

According to QY results, only sample **5** exhibits luminescent conditions to be used as phosphor converter. At this point, the next step is to check its behaviour when pumped in direct contact with the blue LED. To do this, two LEDs where prepared for testing by depositing on to a conventional 450 nm-LED LXML-PR01 from Lumileds a mixture of sample **5** and OE 6531 DOW Corning encapsulant with two different concentrations: 9.5 %, for white emission, and 17.3 %, for yellow emission (full blue photon conversion). Electroluminescent spectra of these devices were measured by biasing at a constant current level of 50 mA. Prior to phosphor deposition, as reference, the pumping signal was also acquired under similar conditions. The results can be observed in Figure 9. The devices fabricated show a clear modification of the spectral shape by compared to photoluminescence (PL) spectrum observed in Figure 8, with a higher contribution of the yellow-red region. Additional PL measurements by externally pumping sample **5** revealed that the spectrum kept the shape at λ_{ex} in the range 340 - 450 nm. Therefore, the variation of the spectral shape is related to thermal issues. On one hand, the junction temperature in conventional LED-dyes typically can range between 50 - 100ºC, depending on operation conditions. On the other, given that sample **5** has an emission quantum efficiency of 50 %, this means that approximately the same portion of absorbed light is transformed into heat, thereby contributing to increase even more the operating temperature.

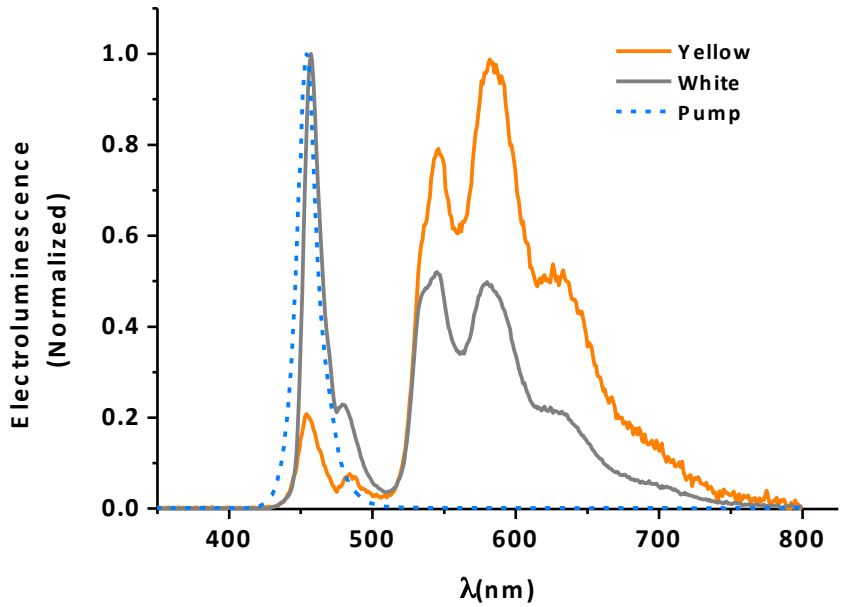

Figure 9. Normalized electroluminescence spectra of pumping source prior to dopant **5** deposition (dashed- blue), yellow emission (solid orange) and white emission (solid grey).

It is worth noting that any increase of the junction temperature translates into thermal expansion of the LED-chip and a subsequent reduction of the energy bandgap. This effect is shown in Figure 9, where a 3-nm red-shift of the blue peak is observed between the reference and the device with the lower concentration (grey solid-line). According to Lumileds specs, this shift represents an increase in Tj of about 100ºC, which can represent a limitation in device reliability. In terms of chromaticity, it is clear from the spectra that phosphor addition induces evident changes colour. This can be clearly seen in the chromaticity diagram shown in Figure 10 (a). The emission from the almost monochromatic LED (colour coordinates x= 0.1507, y= 0.0263) shifts, by addition of a 9.5 % rich encapsulant, to the central region (white region, x= 0.3456, y= 0.3585) of the colour map. The contribution around 450 nm still is quite strong in this device, and in combination with the phosphor emission generates white emission with a CCT of 5006 K. Figure 13 (c) shows an image of such emission. When the phosphor concentration is further increased up to 17.3 % the blue emission from the LED dye gets almost completely quenched (full photon conversion). In this manner, the colour of the emission is practically dominated by the phosphor, resulting in the yellowish emission observed in Figure 13 (d) (x= 0.4690, y= 0.4681).

Nevertheless, it is clear that further studies are needed in order to obtain better controllability of emission properties and improved quantum efficiency and to assure reproducibility of device fabrication and reliability under long operation times.

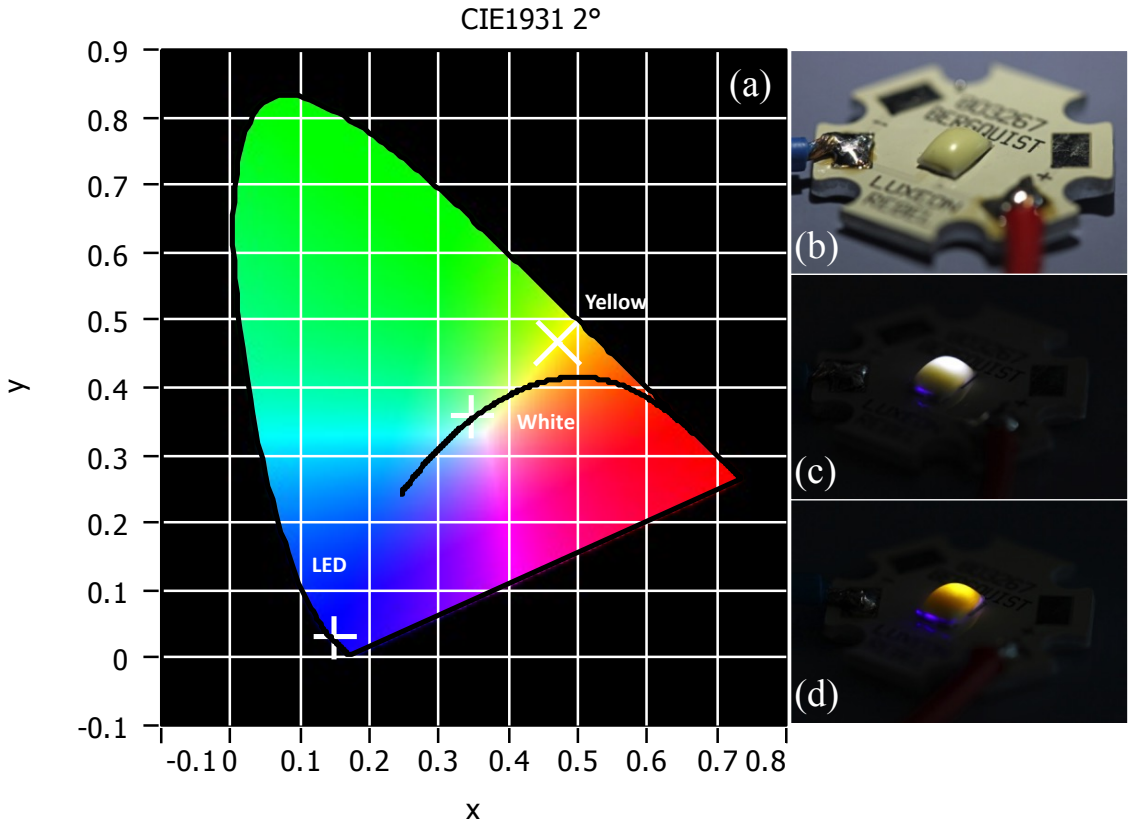

Figure 10. Colorimetric analysis of the three different LEDs (a). Note how the emission from the (almost) monochromatic LED (coordinates x= 0.1507, y= 0.0263) clearly shifts to the white region (x= 0.3456, y= 0.3585) by adding a 9.5 % phosphor **5** mixture and, subsequently, changes into yellow (x= 0.4690, y= 0.4681) by increasing the concentration up to 17.3 %. (b), (c) and (d) show one of the prepared LEDs in off state, the device with white emission and the one emitting in the yellow range, respectively.

CONCLUSIONS

For the first time, this [{Pt(μ-Cl)(η^3-2-Me-C_3H_4)}$_2$] complex has been used to achieve the two-step process: coordination of N-heterocyclic carbenes [PtCl(η^3-2-Me-C_3H_4)(HC^C*-κC*)](**3**) and its subsequent cycloplatination [{Pt(μ-Cl)(C^C*)}$_2$] (**4**). In this new NHC cyclometallated derivative (**4**), the chloro bridge atom can be easily removed to afford two vacant coordination sites, that will put forward a more versatile and accessible pathway to prepare heteroleptic complexes [Pt(C^C*)LL'] containing the "Pt(C^C*)" moiety.

Compounds [Pt(C^C*)(L-*O,O'*)] (**5**-**7**) were prepared by reaction of **4** with the corresponding β-diketonate thallium (I) derivatives. All of them are practically planar, **5** and **6** arrange themselves in pairs through Pt-Pt (3.392 Å (**5**), 3.254 Å (**6**)) and π -π (~ 3.35 Å) interactions. However, complex **7** does not exhibit short Pt-Pt interactions, the molecules stack into pairs showing weak π -π (~ 3.7 Å) interactions between the imidazole and the naphthyl and acac systems.

In glassy solutions, all compounds show structured emissions attributed to ^{3}LL'CT [π(NHC) → π*(R-acac)]/ ML'CT [5d(Pt) → π*(R-acac)] transitions with some ^{3}ILCT (NHC) character in **5**, characteristics of monomeric species. Besides, complex **7** show an additional band at lower energies assigned to ^{3}ππ* excimers upon excitation at λ > 360 nm. In the solid state, while compound **5** shows no effect of the Pt-Pt nor π -π interactions in its emission band compared to that obtained in solution, complexes **6** and **7** display very weak broad band with short lifetime, which is attributed to ^{3}MMLCT [dσ*(Pt) → π*] and/or ^{3}ππ* excited states in aggregates.

Complex **5** exhibits a good PL quantum yield (*Φ, ca*. 0.53) in the solid state, whereas **6** and **7** are extremely poor emitters. It seems that the efficiency experiences an enormous quench with electron-withdrawing R-substituents in the ancillary ligand β-diketonate, probably because they facilitate the formation of aggregates through intermolecular interactions.

Experiments for white-LEDs applications were performed using **5**. It showed that the emission from the almost monochromatic LED (colour coordinates x= 0.1507, y= 0.0263) shifts, by addition of the phosphor **5**, (9.5 % rich encapsulant) to the central region (white region, x= 0.3456, y= 0.3585) of the colour map. The contribution around

450 nm still is quite strong in this device, and in combination with the phosphor emission generates white emission with a CCT of 5006 K.

EXPERIMENTAL SECTION

General Comments. Information describing materials, instrumental methods used for characterization, photophysical and spectroscopic studies, computational details concerning TD-DFT calculations and X-ray structures are contained in the Supporting Information. All chemicals were used as supplied unless stated otherwise. [{Pt(η^3-2-Me-C_3H_4)(μ-Cl)}$_2$][22a] and Tl(hfacac)[39] were prepared following the corresponding literature procedures.

1-(naphthalen-2-yl)-1*H*-imidazole (1).[20-21] The synthetic method followed was similar to a previously reported publication.[19] A mixture of 2-bromonaphthalene (670.5 mg, 3.24 mmol), imidazole (365.0 mg, 5.36 mmol), Cu_2O (75 mg, 0.53 mmol), KOH (403 mg, 7.18 mmol) and DMSO (6 mL) was stirred at 110ºC for 48 h under Ar atmosphere. The cooled reaction mixture was diluted with ethyl acetate (80 mL) and filtered through Celites. The resulting solution was washed with brine (30 mL) and water (30 mL) then dried with anhydrous $MgSO_4$ and evaporated to dryness. The crude product was purified by column chromatography on silica gel using ethyl acetate / methanol (9:1) as eluent to give **1** as a pure white solid. Yield: 420 mg, 67%. ^{1}H NMR (300 MHz, DMSO-d^6, 25ºC): δ = 8.41 (s, 1H, H_1), 8.21 (d, $^4J_{H14\text{-}H6}$ = 2.1, H_{14}), 8.09 (d, $^3J_{H7\text{-}H6}$ = 9.0, H_7), 7.98 (m, 2H, H_9, H_{12}), 7.90 (s, 1H, Im), 7.86 (dd, $^3J_{H6\text{-}H7}$ = 9.0; $^4J_{H6\text{-}H14}$ = 2.1, H_6), 7.57 (m, 2H, H_{10}, H_{11}), 7.16 (s, 1H, Im).

3-methyl-1-(naphthalen-2-yl)-1*H*-imidazolium iodide (2). Methyl iodide (0.2 mL, 3.22 mmol) was added to a solution of **1** (420 mg, 2.15 mmol) in THF (10 mL) under Ar atmosphere. The resulting mixture was refluxed for 16 h to afford a white solid. The solvent was removed in vacuo and diethylether (10 mL) was added to the residue to give **2** as a pure solid. Yield: 670 mg, 93%. ^{1}H NMR (300 MHz, DMSO-d^6, 25ºC): δ 9.88 (s, H_1), 8.42 (s, br, H_2), 8.38 (d, $^4J_{H14\text{-}H6}$ = 2.1, H_{14}), 8.24 (d, $^3J_{H7\text{-}H6}$ = 9.0, H_7), 8.07 (m, 2H, H_9, H_{12}), 8.00 (s, br H_3), 7.88 (dd, $^3J_{H6\text{-}H7}$ = 9.0; $^4J_{H6\text{-}H14}$ = 2.1, H_6), 7.69 (m, 2H, H_{10}, H_{11}), 3.99 (s, 3H, Me (Im)).

Preparation of [PtCl(η^3-2-Me-C_3H_4)(HC^C*-κC*)] (3) (HC^C*-κC* = 3-methyl-1-(naphthalen-2-yl)-1*H*-imidazol-2-ylidene). Silver (I) oxide (157.3 mg, 0.68 mmol) was added to a solution of **2** (456.5 mg, 1.36 mmol) in dry dichloromethane (50 mL) under Ar atmosphere. After 2 h stirring at room temperature, [{Pt(η^3-2-Me-C_3H_4)(μ-Cl)}$_2$] (375 mg, 0.65 mmol) was added to the mixture and left to react 3 h to give a

yellow precipitated (AgI) which was separated by filtration through Celites under Ar. The resulting yellow solution was evaporated to dryness and treated with *n*-hexane (3 x 15 mL) to afford **3** as a pale yellow solid. Yield: 507 mg, 75%. ^{1}H NMR plus HMBC and HSQC (400 MHz, CD_2Cl_2, 25ºC): δ 8.16 (s, H_{14}), 7.94 (m, 4H, $H_{6,7,9,12}$), 7.58 (m, 2H, $H_{10,11}$), 7.36 (d, $^{3}J_{H2\text{-}H3}$ = 2.0, $^{4}J_{H\text{-}Pt}$ = 14.0, H_2), 7.19 (d, $^{3}J_{H3\text{-}H2}$ = 2.0, $^{4}J_{H\text{-}Pt}$ = 10.0, H_3), 3.97 (s, 3H, Me (NHC)), 3.59 (m, 1H$_{syn}$, η^3-2-Me-C_3H_4), 2.61 (m, $^{2}J_{H\text{-}Pt}$ = 28.4, 1H$_{syn}$, η^3-2-Me-C_3H_4), 2.32 (m, $^{2}J_{H\text{-}Pt}$ = 34.0, 1H$_{anti}$, η^3-2-Me-C_3H_4), 1.60 (s, $^{3}J_{H\text{-}Pt}$ = 64.8, 3H, Me, η^3-2-Me-C_3H_4), 1.38 (m, 1H$_{anti}$, η^3-2-Me-C_3H_4). ^{13}C{^{1}H} NMR plus HMBC and HSQC (100.6 MHz, CD_2Cl_2, 25ºC): δ = 176.4 (s, C_1), 137.9 (s, C_5), 132.8 (s, C_8), 132.4 (s, C_{13}), 128.5 (s, C_6), 127.9,127.7 (s, 2C, $C_{9,12}$), 126.9, 126.6 (s, 2C, $C_{10,11}$), 123.9 (s, C_7), 123.2 (s, C_{14}), 122.5 (s, $^{3}J_{C\text{-}Pt}$ = 41.0, C_3), 121.1 (s, $^{3}J_{C\text{-}Pt}$ = 44.2, C_2), 117.7 (s, $^{1}J_{C\text{-}Pt}$ = 70.0, C$^{2'}$, η^3-2-Me-C_3H_4), 57.1 (s, $^{1}J_{C\text{-}Pt}$ = 76.7, C$^{1'}$, η^3-2-Me-C_3H_4), 37.7 (s, C_4 (Me), NHC)), 36.3 (s, C$^{3'}$, η^3-2-Me-C_3H_4), 22.7 (s, $^{2}J_{C\text{-}Pt}$ = 40.2, C$^{4'}$ (Me), η^3-2-Me-C_3H_4); ^{195}Pt{^{1}H} NMR (85.6 MHz, CD_2Cl_2, 25ºC): δ = - 4457; IR (ATR, cm^{-1}): ν = 280 (s, Pt-Cl); MS-ESI (+): m/z: 666.4 [Pt(η^3-2-Me-C_3H_4)(HC^C*,-κC*)$_2$]$^{+}$; elemental analysis calcd (%) for $C_{18}H_{19}N_2ClPt$: C 43.77, H 3.87, N 5.67; found: C 43.99, H 3.96, N 5.56.

Preparation of [{Pt(*μ*-Cl)(C^C*)}$_2$] (4). Compound **3** (510 mg, 1.03 mmol) was dissolved in 2-methoxyethanol (10 mL) and refluxed for 4 h. The resultant grey suspension was filtered and the solid was washed with dichloromethane (2 x 5 mL) and diethyl ether (2 x 5 mL). The solid was treated with activated carbon in hot MeCN (60 mL) and filtered through Celites. The solution was evaporated to dryness and diethyl ether (10 mL) was added to the residue. The remaining solid was filtered and dried (110ºC) to give pure **4** as a white solid. Yield: 272 mg, 60%. ^{1}H NMR (300 MHz, DMSO-*d*^{6}, 25ºC): δ = 8.85 (s, $^{3}J_{H\text{-}Pt}$ = 62.7, H_7), 8.26 (d, $^{3}J_{H2\text{-}H3}$ = 1.5, H_2), 7.93 (s, H_{14}), 7.79 (d, $^{3}J_{H\text{-}H}$ = 7.8, H_9), 7.71 (d, $^{3}J_{H\text{-}H}$ = 7.8, H_{12}), 7.61 (d, $^{3}J_{H3\text{-}H2}$ = 1.5, H_3), 7.44 (m, 2H, $H_{10,11}$), 4.23 (s, 3H, Me (NHC)); ^{13}C{^{1}H} NMR plus HMBC and HSQC (75.4 MHz, DMSO-*d*^{6}, 25ºC): δ = 156.1 (s, C_1), 145.4 (s, C_6), 133.6 (s, C_7), 132.4 (s, C_{13}), 131.5 (s, C_8), 127.7 (s, C_9), 127.5 (s, C_{12}), 126.1 (s, C_5), 126.0 (s, C_3), 125.6 (s, 2C, $C_{10,11}$), 115.6 (s, $^{3}J_{C\text{-}Pt}$ = 45.0, C_2), 108.6 (s, $^{3}J_{C\text{-}Pt}$ = 30.0, C_{14}), 38.2 (s, C_4,(Me), NHC); HMQC ^{1}H-^{195}Pt NMR (300 MHz, DMSO-*d*^{6}, 25ºC): δ = - 3506; IR (ATR, cm^{-1}): ν = 271 (s, Pt-Cl); elemental analysis calcd (%) for $C_{14}H_{11}N_2ClPt$: C 38.41, H 2.53, N 6.39; found: C 38.23, H 2.48, N 6.51.

Preparation of [Pt(C^C*)(acac)] (5). Tlacac (270 mg, 0.89 mmol) was added to a white suspension of **1** (400 mg, 0.91 mmol) in dichloromethane (40 mL) at r.t. After 2 h stirring, the resulting mixture was filtered through Celites and evaporated to dryness. Addition of methanol (3 x 5 mL) to the residue rendered a solid which was recrystallized by redissolving in 15 mL of dichloromethane/diethyl ether (1:1), filtering through celites and evaporating to dryness. Addition of methanol (3 x 5 mL) to the residue rendered **5** as a pure white solid. Yield: 320 mg, 71%. ^{1}H NMR (400 MHz, CD_2Cl_2, 25ºC): δ = 8.06 (s, $^{3}J_{H\text{-}Pt}$ = 57.2, H_7), 7.78 (m, H_9), 7.71 (m, H_{12}), 7.42 (d, $^{3}J_{H\text{-}H}$ = 2.0, H_2), 7.34 (m, 3H, $H_{10,11,14}$), 6.89 (d, $^{3}J_{H\text{-}H}$ = 2.0, H_3), 5.56 (s, C-H, acac), 4.07 (s, 3H, Me (NHC)), 2.12 (s, 3H, Me (acac)), 1.99 (s, 3H, Me (acac)); $^{13}C\{^{1}H\}$ NMR plus HMBC and HSQC (100.6 MHz, CD_2Cl_2, 293 K): δ = 185.2 and 185.1 (s, C=O, acac), 150.6 (s, C_1), 146.3 (s, C_6), 131.6 (s, C_{13}), 131.4 (s, C_8), 129.4 (s, C_7), 127.2 (s, C_{12}), 126.9 (s, C_9), 124.7 (s, C_{11}), 124.2 (s, C_{10}), 124.0 (s, C_5), 121.8 (s, $^{3}J_{C\text{-}Pt}$ = 46.8, C_3), 114.2 (s, $^{3}J_{C\text{-}Pt}$ = 52.8, C_2), 106.4 (s, $^{3}J_{C\text{-}Pt}$ = 33.8, C_{14}), 101.7 (s, $^{3}J_{C\text{-}Pt}$ = 56.4, C-H(acac)), 34.8 (s, C_4 (Me), NHC), 27.7 (s, Me (acac)), 27.6 (s, Me (acac)); $^{195}Pt\{^{1}H\}$ NMR (64.3 MHz, CD_2Cl_2, 293 K): δ = - 3360; IR (ATR, cm^{-1}): ν =1518 (s, C=C); 1557 and 1575 (s, C=O); MS MALDI (+): m/z: 501.2 $[M]^+$; elemental analysis calcd (%) for $C_{19}H_{18}N_2O_2Pt$: C 45.51, H 3.61, N 5.58; found: C 45.30, H 3.77, N 5.38.

Preparation of [Pt(C^C*)(phacac)] (6). It was prepared following the method described for **5**. Tl(phacac) (193.0 mg, 0.45 mmol) and **4** (202.1 mg, 0.46 mmol). **6** (207.2 mg, 73%). ^{1}H NMR (400 MHz, CD_2Cl_2, 25ºC): δ = 8.25 (s, $^{3}J_{H\text{-}Pt}$ = 55.2, H_7), 8.21 (d, $^{3}J_{H\text{-}H}$ = 8.4, $2H_{ortho}$, phacac), 7.96 (d, $^{3}J_{H\text{-}H}$ = 8.4, $2H_{ortho}$, phacac), 7.84 (m, H_9), 7.73 (m, H_{12}), [7.64-7.53] (m, $2H_{para}$, $2H_{meta}$, phacac), 7.45 (m, 3H, H_2 (NHC) and $2H_{meta}$ (phacac)), 7.37 (m, 3H, $H_{10,11,14}$), 6.91 (d, $^{3}J_{H\text{-}H}$ = 2.4, H_3 (NHC)), 6.82 (s, C-H, phacac), 4.16 (s, 3H, Me (NHC)); $^{13}C\{^{1}H\}$ NMR plus HMBC and HSQC (100.6 MHz, CD_2Cl_2, 293 K): δ = 180.6 and 179.4 (s, C=O, phacac), 150.3 (s, C_1), 146.3 (s, C_6), 140.9 and 139.8 (s, C_{ipso}(phacac)), 131.6 (s, C_{13}), 131.5 (s, C_8), 130.9 and 130.6 (s, C_{para}(phacac)), 129.8 (s, C_7), 128.6 and 128.5 (s, C_{meta}(phacac)), [127.2-126.9] (s, 6C, $C_{9,12}$, C_{ortho}(phacac)), 124.7and 124.3(s, $C_{10,11}$), 123.6 (s, C_5), 121.8 (s, C_3), 114.3 (s, C_2), 106.6 (s, C_{14}), 96.9 (s, C-H(phacac)), 35.2 (s, C_4 (Me), NHC); $^{195}Pt\{^{1}H\}$ NMR (64.3 MHz, CD_2Cl_2, 293 K): δ = - 3296; IR (ATR, cm^{-1}): ν = 1522 (s, C=C); 1539 and 1590 (s, C=O); MS MALDI (+): m/z: 625.3 $[M]^+$; elemental analysis calcd (%) for $C_{29}H_{22}N_2O_2Pt$: C 55.67, H 3.54, N 4.47; found: C 55.04, H 3.94, N 4.62.

Preparation of [Pt(C^C*)(hfacac)] (7). It was prepared following the method described for **5**. Tl(hfacac) (187.0 mg, 0.45 mmol) and **4** (200.1 mg, 0.45 mmol). **7** (202.2 mg, 72%). ^{1}H NMR (400 MHz, CD_2Cl_2, 25ºC): δ = 7.79 (s, $^{3}J_{H\text{-}Pt}$ = 60.0, H_7), 7.74 (m, 2H, $H_{9,12}$), 7.37 (m, 2H, $H_{10,11}$), 7.36 (d, $^{3}J_{H\text{-}H}$ = 2.0, H_2), 7.32 (s, $^{3}J_{H\text{-}Pt}$ = 15.2, H_{14}), 6.84 (d, $^{3}J_{H\text{-}H}$ = 2.0, H_3), 6.26 (s, C-H, hfacac), 3.86 (s, 3H, Me (NHC)); ^{13}C{^{1}H} NMR plus HMBC and HSQC (100.6 MHz, CD_2Cl_2, 25ºC): δ = 171.6 and 171.5 (s, C=O, hfacac), 145.4 (s, C_1), 145.3 (s, C_6), 131.8 (s, C_{13}), 131.7 (s, C_8), 130.0 (s, C_7), 127.2 (s, 2C, $C_{12,9}$), 125.1 and 125.0 (s, $C_{11,10}$), 122.5 (s, C_5), 122.2 (s, C_3), 117. 4 and 117.8 (CF_3, (hfacac)), 114.4 (s, C_2), 107.2 (s, C_{14}), 93.5 (s, C-H(hfacac)), 35.0 (s, C_4 (Me), NHC); ^{19}F{^{1}H} NMR (282.4 MHz, CD_2Cl_2, 25ºC): δ = -75.5 (s, CF_3 (hfacac)), -75.8 (s, CF_3 (hfacac)); ^{195}Pt{^{1}H} NMR (64.3 MHz, CD_2Cl_2, 25ºC): δ = - 3232; IR (ATR, cm^{-1}): ν = 1615 (s, C=O); MS MALDI (+): m/z: 609.1 $[M]^+$; elemental analysis calcd (%) for $C_{19}H_{12}N_2O_2F_6Pt$: C 37.44, H 1.98, N 4.59; found: C 37.33, H 1.77, N 4.58.

Acknowledgments: This work was supported by the Spanish MICINN (DGPTC/FEDER) (Project CTQ2008-06669-C02-01/BQU), MINECO (CTQ2012-35251 and TEC2012-38901-C02-01), the Gobierno de Aragón (Grupo Consolidado E21: Química Inorgánica y de los Compuestos Organometálicos) and the ARAID-EU program (Ref. 246558; FP7-PEOPLE-COFUNF-2008). The authors thank the Centro de Supercomputación de Galicia (CESGA) for generous allocation of computational resources.

Supporting information available: General procedures, computational and crystallographic details. Xray structure analysis of **5** **0.5·CH_2Cl_2** **6** and **7** (Table S1). NMR spectra (Fig. S1-S4). X-ray structures (Fig. S5 and S6). UV-Vis data (Table S2, Fig. S7 and S8). Tables of atomic coordinates of compounds (S3 - S5). Pictures of the representative frontier orbitals for **5-7** (Figure S9-S11). UV-vis spectra and calculated transitions in CH_2Cl_2 (Figures S12- S14). Emission spectra (Fig. S15 and S16). TGA (Fig. S17). Crystallographic data in CIF format.

REFERENCES

[1] U. S. D. o. Energy, *"Multi-Year Program Plan"* **2013**.

[2] N. R. E. L. (NREL), *"Amber LEDs for Solid-State Lighting: White light with unprecedented efficiencies"* **2013**.

[3] U. S. D. o. Energy, *"Critical Materials Strategy"* **2011**.

[4] a) L. Murphy, J. A. G. Williams, *Top. Organomet. Chem.* **2010**, *28*, 75-111; b) J. A. Gareth Williams, *Top. Curr. Chem.* **2007**, *281*, 205-268; c) G. Zhou, Q. Wang, X. Wang, C.-L. Ho, W.-Y. Wong, D. Ma, L. Wang, Z. Lin, *Journal of Materials Chemistry* **2010**, *20*, 7472-7484.

[5] a) Q. Zhao, F. Li, C. Huang, *Chem. Soc. Rev.* **2010**, *39*, 3007-3030; b) K. M.-C. Wong, M. M.-Y. Chan, V. W.-W. Yam, *Adv. Mat.* **2014**, 26, 5558-5568; c) S. D. Taylor, W. Howard, N. Kaval, R. Hart, J. A. Krause, W. B. Connick, *Chem. Commun.* **2010**, *46*, 1070-1072.

[6] a) P. Wang, C. H. Leung, D. L. Ma, R. W. Y. Sun, S. C. Yan, Q. S. Chen, C. M. Che, *Angew Chem Int Ed* **2011**, *50*, 2554-2558; b) P. Wang, C. H. Leung, D. L. Ma, W. Lu, C. M. Che, *Chem-Asian J.* **2010**, *5*, 2271-2280; c) C. K. Koo, K. L. Wong, C. W. Y. Man, Y. W. Lam, K. Y. So, H. L. Tam, S. W. Tsao, K. W. Cheah, K. C. Lau, Y. Y. Yang, J. C. Chen, M. H. W. Lam, *Inorg. Chem.* **2009**, *48*, 872-878.

[7] a) J. A. G. Williams, S. Develay, D. L. Rochester, L. Murphy, *Coord. Chem. Rev.* **2008**, *252*, 2596-2611; b) J. A. G. Williams, in *Top. Organomet. Chem., Vol. 28* (Eds.: H. Bozec, V. Guerchais), Springer, New York, **2009**.

[8] T. Sajoto, P. I. Djurovich, A. Tamayo, M. Yousufuddin, R. Bau, M. E. Thompson, R. J. Holmes, S. R. Forrest, *Inorg. Chem.* **2005**, *44*, 7992-8003.

[9] a) X. Bugaut, F. Glorius, *Chem. Soc. Rev.* **2012**, *41*, 3511-3522; b) G. C. Fortman, S. P. Nolan, *Chem. Soc. Rev.* **2011**, *40*, 5151-5169; c) S. T. Liddle, I. S. Edworthy, P. L. Arnold, *Chem. Soc. Rev.* **2007**, *36*, 1732-1744; d) W. A. Herrmann, *Angew. Chem. Int. Ed.* **2002**, *41*, 1290-1309; e) O. Kuhl, *Chem. Soc. Rev.* **2007**, *36*, 592-607.

[10] a) I. J. B. Lin, C. S. Vasam, *J. Organomet. Chem.* **2005**, *690*, 3498-3512; b) R. T. W. Huang, W. C. Wang, R. Y. Yang, J. T. Lu, I. J. B. Lin, *Dalton Trans.* **2009**, 7121-7131; c) C. K. Lee, C. S. Vasam, T. W. Huang, H. M. J. Wang, R. Y. Yang, C. S. Lee, I. J. B. Lin, *Organometallics* **2006**, *25*, 3768-3775.

[11] a) A. Melaiye, Z. H. Sun, K. Hindi, A. Milsted, D. Ely, D. H. Reneker, C. A. Tessier, W. J. Youngs, *J. Am. Chem. Soc.* **2005**, *127*, 2285-2291; b) K. M. Hindi, M. J. Panzner, C. A. Tessier, C. L. Cannon, W. J. Youngs, *Chem. Rev.* **2009**, *109*, 3859-3884; c) H. G. Raubenheimer, S. Cronje, *Chem. Soc. Rev.* **2008**, *37*, 1998-2011; d) L. Mercs, M. Albrecht, *Chem. Soc. Rev.* **2010**, *39*, 1903-1912.

[12] a) V. W. W. Yam, E. C. C. Cheng, in *Photochemistry and Photophysics of Coordination Compounds Ii, Vol. 281* (Eds.: V. Balzani, S. Campagna), Springer-Verlag Berlin, Berlin, **2007**, pp. 269-309; b) S. J. Hock, L.-A. Schaper, W. A. Herrmann, F. E. Kuhn, *Chem. Soc. Rev.* **2013**, *42*, 5073-5089; c) S. U. Son, K. H. Park, Y. S. Lee, B. Y. Kim, C. H. Choi, M. S. Lah, Y. H. Jang, D. J. Jang, Y. K. Chung, *Inorg. Chem.* **2004**, *43*, 6896-6898; d) Y. Unger, A. Zeller, S. Ahrens, T. Strassner, *Chem. Commun.* **2008**, 3263-3265; e) R. J. Holmes, S. R. Forrest, T. Sajoto, A. Tamayo, P. I. Djurovich, M. E. Thompson, J. Brooks, Y. J. Tung, B. W. D'Andrade, M. S. Weaver, R. C. Kwong, J. J. Brown, *Appl. Phys. Lett.* **2005**, *87*; f) C. F. Chang, Y. M. Cheng, Y. Chi, Y. C. Chiu, C. C.

Lin, G. H. Lee, P. T. Chou, C. C. Chen, C. H. Chang, C. C. Wu, *Angew. Chem. Int. Ed.* **2008**, *47*, 4542-4545; g) C. H. Hsieh, F. I. Wu, C. H. Fan, M. J. Huang, K. Y. Lu, P. Y. Chou, Y. H. O. Yang, S. H. Wu, I. C. Chen, S. H. Chou, K. T. Wong, C. H. Cheng, *Chem. Eur. J.* **2011**, *17*, 9180-9187; h) H. Sasabe, J. Takamatsu, T. Motoyama, S. Watanabe, G. Wagenblast, N. Langer, O. Molt, E. Fuchs, C. Lennartz, J. Kido, *Adv. Mat.* **2010**, *22*, 5003-+; i) K. Y. Lu, H. H. Chou, C. H. Hsieh, Y. H. O. Yang, H. R. Tsai, H. Y. Tsai, L. C. Hsu, C. Y. Chen, I. C. Chen, C. H. Cheng, *Adv. Mat.* **2011**, *23*, 4933-4937; j) R. Visbal, I. Ospino, J. M. Lopez-de-Luzuriaga, A. Laguna, M. C. Gimeno, *J. Am. Chem. Soc.* **2013**, *135*, 4712-4715.

[13] a) S. Haneder, E. Da Como, J. Feldmann, J. M. Lupton, C. Lennartz, P. Erk, E. Fuchs, O. Molt, I. Munster, C. Schildknecht, G. Wagenblast, *Adv. Mater.* **2008**, *20*, 3325-+; b) Y. Unger, D. Meyer, O. Molt, C. Schildknecht, I. Münster, G. Wagenblast, T. Strassner, *Angew. Chem. Int. Ed.* **2010**, *49*, 10214-10216; c) Z. M. Hudson, C. Sun, M. G. Helander, Y. L. Chang, Z. H. Lu, S. N. Wang, *J. Am. Chem. Soc.* **2012**, *134*, 13930-13933; d) X. F. Zhang, A. M. Wright, N. J. DeYonker, T. K. Hollis, N. I. Hammer, C. E. Webster, E. J. Valente, *Organometallics* **2012**, *31*, 1664-1672; e) A. Tronnier, A. Risler, N. Langer, G. Wagenblast, I. Munster, T. Strassner, *Organometallics* **2012**, *31*, 7447-7452; f) A. Tronnier, S. Metz, G. Wagenblast, I. Muenster, T. Strassner, *Dalton Trans.* **2014**, *43*, 3297-3305; g) A. Tronnier, N. Nischan, S. Metz, G. Wagenblast, I. Muenster, T. Strassner, *Eur. J. Inorg. Chem.* **2014**, *2014*, 256-264; h) A. Tronnier, A. Poethig, E. Herdtweck, T. Strassner, *Organometallics* **2014**, *33*, 898-908; i) A. Tronnier, N. Nischan, T. Strassner, *J. Organomet. Chem.* **2013**,

730, 37-43; j) X. Zhang, B. Cao, E. J. Valente, T. K. Hollis, *Organometallics* **2013**, *32*, 752-761.

[14] Z. M. Hudson, B. A. Blight, S. N. Wang, *Org. Lett.* **2012**, *14*, 1700-1703.

[15] a) D. N. Kozhevnikov, V. N. Kozhevnikov, M. Z. Shafikov, A. M. Prokhorov, D. W. Bruce, J. A. G. Williams, *Inorg. Chem.* **2011**, *50*, 3804-3815; b) D. A. K. Vezzu, J. C. Deaton, J. S. Jones, L. Bartolotti, C. F. Harris, A. P. Marchetti, M. Kondakova, R. D. Pike, S. Q. Huo, *Inorg. Chem.* **2010**, *49*, 5107-5119; c) A. F. Rausch, L. Murphy, J. A. G. Williams, H. Yersin, *Inorg. Chem.* **2011**, *51*, 312-319; d) Y. You, J. n. Seo, S. H. Kim, K. S. Kim, T. K. Ahn, D. Kim, S. Y. Park, *Inorg. Chem.* **2008**, *47*, 1476-1487; e) Y. You, K. S. Kim, T. K. Ahn, D. Kim, S. Y. Park, *J. Phys. Chem. C* **2007**, *111*, 4052-4060; f) A. J. Wilkinson, H. Puschmann, J. A. K. Howard, C. E. Foster, J. A. G. Williams, *Inorg. Chem.* **2006**, *45*, 8685-8699; g) J. Brooks, Y. Babayan, S. Lamansky, P. I. Djurovich, I. Tsyba, R. t. Bau, M. E. Thompson, *Inorg. Chem.* **2002**, *41*, 3055-3066.

[16] a) J. Fornies, S. Fuertes, J. A. Lopez, A. Martin, V. Sicilia, *Inorg. Chem.* **2008**, *47*, 7166-7176; b) K. Zhang, J. Hu, K. C. Chan, K. Y. Wong, J. H. K. Yip, *Eur. J. Inorg. Chem.* **2007**, 384-393.

[17] a) S. Fernández, J. Forniés, B. Gil, J. Gómez, E. Lalinde, *Dalton Trans.* **2003**, 822-830; b) A. Diez, J. Fornies, S. Fuertes, E. Lalinde, C. Larraz, J. A. Lopez, A. Martin, M. T. Moreno, V. Sicilia, *Organometallics* **2009**, *28*, 1705-1718; c) J. Forniés, S. Fuertes, A. Martin, V. Sicilia, B. Gil, E. Lalinde, *Dalton Trans.* **2009**, 2224-2234; d) A. Díez, J. Fornies, C. Larraz, E. Lalinde, J. A. López, A. Martin, M. T. Moreno, V. Sicilia, *Inorg. Chem.* **2010**, *49*, 3239-3259; e) J. Fornies, V. Sicilia, P. Borja, J. M. Casas, A. Diez, E. Lalinde, C. Larraz, A. Martin, M. T. Moreno, *Chem-Asian J.* **2012**, *7*, 2813-2823.

[18] a) J. Fornies, V. Sicilia, C. Larraz, J. A. Camerano, A. Martin, J. M. Casas, A. C. Tsipis, *Organometallics* **2010**, *29*, 1396-1405; b) V. Sicilia, S. Fuertes, A. Martin, A. Palacios, *Organometallics* **2013**, *32*, 4092-4102.

[19] Y. Z. Huang, H. Miao, Q. H. Zhang, C. Chen, J. Xu, *Catal. Lett.* **2008**, *122*, 344-348.

[20] M. C. Perry, X. Cui, M. T. Powell, D.-R. Hou, J. H. Reibenspies, K. Burgess, *J. Am. Chem. Soc.* **2002**, *125*, 113-123.

[21] E. Alcalde, I. Dinares, S. Rodriguez, C. G. de Miguel, *Eur. J. Org. Chem.* **2005**, 1637-1643.

[22] a) D. J. Mabbott, B. E. Mann, P. M. Maitlis, *J. Chem. Soc., Dalton Trans.* **1977**, 294-299; b) B. E. Mann, B. L. Shaw, G. Shaw, *J. Chem. Soc. A* **1971**, 3536-&.

[23] a) H. Cerfontain, *Interscience monographs on organic chemistry* **1968**, 68-69; b) F. A. Carey, R. J. Sundberg, *Adv. Org. Chem., 2nd ed.; Plenum Press: New York; Part B* **1984**, 416.

[24] J. March, *Adv. Org. Chem., 3rd ed.; Wiley Interscience: New York* **1985**, 461.

[25] R. T. Morrison, R. N. Boyd, *Organic Chemistry, 5th Ed.* **1987**.

[26] a) J.-M. Valk, F. Maassarani, P. van der Sluis, A. L. Spek, J. Boersma, G. van Koten, *Organometallics* **1994**, *13*, 2320-2329; b) J. M. Valk, R. Vanbelzen, J. Boersma, A. L. Spek, G. Vankoten, *J. Chem. Soc., Dalton Trans.* **1994**, 2293-2302; c) M. Crespo, M. Font-Bardia, S. Perez, X. Solans, *J. Organomet. Chem.* **2002**, *642*, 171-178.

[27] J. C. Bernhammer, H. V. Huynh, *Organometallics* **2013**, *33*, 172-180.

[28] G. L. Petretto, M. Wang, A. Zucca, J. P. Rourke, *Dalton Trans.* **2010**, *39*, 7822-7825.

[29] a) B. Bock, K. Flatau, H. Junge, M. Kuhr, H. Musso, *Angew. Chem. Int. Ed.* **1971**, *10*, 225-235; b) K. Nakamoto, *Angew. Chem. Int. Ed.* **1972**, *11*, 666-674; c) G. T. Behnke, K. Nakamoto, *Inorg. Chem.* **1967**, *6*, 433-440; d) G. T. Behnke, K. Nakamoto, *Inorg. Chem.* **1967**, *6*, 440-445.

[30] M. Tenne, S. Metz, I. Munster, G. Wagenblast, T. Strassner, *Organometallics* **2013**, *32*, 6257-6264.

[31] M. Nardelli, *J. Appl. Crystallogr.* **1995**, *28*, 659-659.

[32] a) V. H. Houlding, V. M. Miskowski, *Coord. Chem. Rev.* **1991**, *111*, 145-152; b) C. A. Hunter, *Chem. Soc. Rev.* **1994**, *23*, 101-109; c) W. B. Connick, R. E. Marsh, W. P. Schaefer, H. B. Gray, *Inorg. Chem.* **1997**, *36*, 913-922; d) L. Chassot, E. Muller, A. Vonzelewsky, *Inorg. Chem.* **1984**, *23*, 4249-4253.

[33] P. Pyykko, *Chem. Rev.* **1997**, *97*, 597-636.

[34] C. Janiak, *J. Chem. Soc., Dalton Trans.* **2000**, 3885-3896.

[35] J. A. G. Williams, *Top. Curr. Chem.* **2007**, *281*, 205-268.

[36] a) A. Martín, U. Belío, S. Fuertes, V. Sicilia, *Eur. J. Inorg. Chem.* **2013**, 2231-2247; b) J. R. Berenguer, A. Díez, J. Fernández, J. Forniés, A. García, B. Gil, E. Lalinde, M. T. Moreno, *Inorg. Chem.* **2008**, *47*, 7703-7716.

[37] a) T. J. Wadas, Q.-M. Wang, Y.-j. Kim, C. Flaschenreim, T. N. Blanton, R. Eisenberg, *J. Am. Chem. Soc.* **2004**, *126*, 16841-16849; b) S. C. F. Kui, S. S. Y. Chui, C. M. Che, N. Y. Zhu, *J. Am. Chem. Soc.* **2006**, *128*, 8297-8309; c) A. Y. Y. Tam, K. M. C. Wong, G. X. Wang, V. W. W. Yam, *Chem. Commun.* **2007**, 2028-2030; d) V. Sicilia, J. Fornies, J. M. Casas, A. Martin, J. A. Lopez, C. Larraz, P. Borja, C. Ovejero, D. Tordera, H. Bolink, *Inorg. Chem.* **2012**, *51*, 3427-3435; e) X. Zhang, J. Y. Wang, J. Ni, L. Y. Zhang, Z. N. Chen, *Inorg. Chem.* **2012**, *51*, 5569-5579.

[38] N. C. George, K. A. Denault, R. Seshadri, *Annu. Rev. Mater. Res.* **2013**, *43*, 481-501.

[39] F. A. Hartman, P. L. Jacoby, A. Wojcicki, *Inorg. Syn.* **1970**, *12*, 81-85.

Table 1. Population Analysis (%) of Frontier MOs in the Ground State for **5**-**7**

MO	eV			Pt			imidazol			Napth			R-acac		
	5	**6**	**7**	**5**	**6**	**7**	**5**	**6**	**7**	**5**	**6**	**7**	**5**	**6**	**7**
L+2	-0.46	-0.55	-0.83	22	16	19	19	13	16	57	47	63	2	24	2
L+1	-0.76	-0.83	-1.14	6	7	10	21	28	33	50	62	55	23	3	2
L	-0.95	-1.62	-2.22	2	2	3	8	1	1	16	1	1	74	96	95
H	-5.14	-5.17	-5.54	21	21	16	0	0	0	69	69	81	10	10	3
H-1	-5.52	-5.55	-5.91	21	22	14	22	21	19	53	52	66	4	5	1
H-2	-5.80	-5.78	-6.43	16	10	33	10	7	26	27	25	14	47	58	27
H-4		-6.28	-7.10		24	25		17	11		14	38		45	26
H-5			-7.39			17			12			34			38

Table 2. Selected singlet excited states calculated by TD-DFT for **5-7** in solution of CH_2Cl_2

	λ_{exc} (calc.)/nm	o.s.	Transition (Percentage contribution, %)
			[Pt(C^C*)(acac)] (5)
S1	338	0.0032	H → L (88); H-1 → L (4); H → L+2 (3)
S2	329	0.0188	H → L+1 (53); H → L+2 (15); H-1 → L (13); H-1→ L +1 (9); H →L (5)
S3	314	0.1583	H-1 → L (46); H → L+1 (31); H-1 → L+2 (13.5); H-1→ L +1 (2.5)
S4	304	0.1092	H -1→ L+1 (35); H-1 → L (30); H → L+2 (17); H-1→ L +2 (10); H →L+1 (4)
			[Pt(C^C*)(phacac)] (6)
S1	402	0.0197	H → L (97)
S2	366	0.1527	H-1 → L (95); H-2 → L (2)
S3	335	0.1232	H-2 → L (93); H-1 → L (2.6)
S4	306	0.3434	H -4→ L (86); H-1 → L+1 (5)
			[Pt(C^C*)(hfacac)] (7)
S1	450	0.0070	H → L (96)
S2	401	0.0761	H-1 → L (96)
S3	325	0.0646	H → L+1 (63); H-1 → L+1 (18); H → L+2 (15)
S4	286	0.1329	H -4→ L (38); H-1 → L+2 (34); H -5→ L (7); H → L+1 (6); H -1→ L+1 (6)

Table 3. Photophysical Data for complexes **5**-**7**.

Comp.	Media (T/K)	λ_{ex} (nm)	λ_{em} (nm)	τ (μs)	ϕ
5	Solid (298)	350-440	534_{max}, 577, 630	35	0.53
	Solid (77)	350-440	534_{max}, 577, 630	53	
	2-MeTHF$_a$ (77)	308, 355_{sh}	474_{max}, 509, 550, 598	408	
	2-MeTHF$_b$ (77)	350	474_{max}, 509, 550, 598	412	
6	Solid (298)	440-500	675	0.1	0.01
	Solid (77)	440-500	685	0.3	
	2-MeTHF$_a$ (77)	310, 344, 372, 390	493_{max}, 530, 568	15	
	2-MeTHF$_b$ (77)	425	497_{max}, 535, 571	19	
7	Solid (298)	350-520	565, 608_{max}, 660	0.3	0.02
	Solid (77)	350-530	558, 608_{max}, 665	1.2	
	2-MeTHF$_a$ (77)	290-330	474_{max}, 508, 549, 592	397	
		370-400	474_{sh}, 543, 580_{max},629	1.6	
	2-MeTHF$_b$ (77)	310-500	543, 580_{max}, 629	1.8	

a = 10^{-5}M; *b* = 10^{-3}M

For the Table of Contents Only

Title: STEPWISE STRATEGY TO CYCLOMETALLATED Pt(II) COM-PLEXES WITH N-HETEROCYCLIC CARBENE LIGANDS. LUMINESCENCE STUDY ON NEW β–DIKETONATE COMPLEXES

Platinum-based phosphors containing a cyclometallated N-heterocyclic carbene (NHC) have been prepared *via* a stepwise process. The suitability of the most efficient compound as a wavelength converter for white-LEDs applications was also evaluated.

*Sara Fuertes, Hector García, Mariano Perálvarez, Wim Hertog, Josep Carreras, Violeta Sicilia**

Keywords: N-heterocyclic carbenes (NHC), platinum (II), cyclometallated compounds, luminescence